Title

Suppression and azimuthal anisotropy of prompt and nonprompt J/ψ production in PbPb collisions at sNN=2.76TeV

Journal

European Physical Journal C, 77(4)

ISSN

1434-6044

Authors

Khachatryan, V

Sirunyan, AM

Tumasyan, A

et al.

Publication Date

2017-04-01

DOI

10.1140/epjc/s10052-017-4781-1

Eur. Phys. J. C (2017) 77:252
DOI 10.1140/epjc/s10052-017-4781-1

THE EUROPEAN PHYSICAL JOURNAL C

Regular Article - Experimental Physics

Suppression and azimuthal anisotropy of prompt and nonprompt J/ψ production in PbPb collisions at $\sqrt{s_{NN}} = 2.76$ TeV

CMS Collaboration*

CERN, 1211 Geneva 23, Switzerland

Received: 3 October 2016 / Accepted: 21 March 2017 / Published online: 19 April 2017

Abstract The nuclear modification factor R_{AA} and the azimuthal anisotropy coefficient v_2 of prompt and nonprompt (i.e. those from decays of b hadrons) J/ψ mesons, measured from PbPb and pp collisions at $\sqrt{s_{NN}} = 2.76$ TeV at the LHC, are reported. The results are presented in several event centrality intervals and several kinematic regions, for transverse momenta $p_T > 6.5$ GeV/c and rapidity $|y| < 2.4$, extending down to $p_T = 3$ GeV/c in the $1.6 < |y| < 2.4$ range. The v_2 of prompt J/ψ is found to be nonzero, but with no strong dependence on centrality, rapidity, or p_T over the full kinematic range studied. The measured v_2 of nonprompt J/ψ is consistent with zero. The R_{AA} of prompt J/ψ exhibits a suppression that increases from peripheral to central collisions but does not vary strongly as a function of either y or p_T in the fiducial range. The nonprompt J/ψ R_{AA} shows a suppression which becomes stronger as rapidity or p_T increases. The v_2 and R_{AA} of open and hidden charm, and of open charm and beauty, are compared.

1 Introduction

Recent data from RHIC and the CERN LHC for mesons containing charm and beauty quarks have allowed more detailed theoretical and experimental studies [1] of the phenomenology of these heavy quarks in a deconfined quark gluon plasma (QGP) [2] at large energy densities and high temperatures [3]. Heavy quarks, whether as quarkonium states $Q\overline{Q}$ (hidden heavy flavour) [4] or as mesons made of heavy-light quark–antiquark pairs $Q\overline{q}$ (open heavy flavour) [5], are considered key probes of the QGP, since their short formation time allows them to probe all stages of the QGP evolution [1].

At LHC energies, the inclusive J/ψ yield contains a significant nonprompt contribution from b hadron decays [6–8], offering the opportunity of studying both open beauty and hidden charm in the same measurement. Because of the long lifetime ($\mathcal{O}(500)\,\mu m/c$) of b hadrons, compared to the QGP lifetime ($\mathcal{O}(10)\,fm/c$), the nonprompt contribution should not suffer from colour screening of the potential between the Q and the $\overline{Q}$ by the surrounding light quarks and gluons, which decreases the prompt quarkonium yield [9]. Instead, the nonprompt contribution should reflect the energy loss of b quarks in the medium. The importance of an unambiguous and detailed measurement of open beauty flavour is driven by the need to understand key features of the dynamics of parton interactions and hadron formation in the QGP: the colour-charge and parton-mass dependences for the in-medium interactions [5,10–13], the relative contribution of radiative and collisional energy loss [14–16], and the effects of different hadron formation times [17,18]. Another aspect of the heavy-quark phenomenology in the QGP concerns differences in the behaviour (energy loss mechanisms, amount and strength of interactions with the surrounding medium) of a $Q\overline{Q}$ pair (the pre-quarkonium state) relative to that of a single heavy quark Q (the pre-meson component) [19–21].

Experimentally, modifications to the particle production are usually quantified by the ratio of the yield measured in heavy ion collisions to that in proton–proton (pp) collisions, scaled by the mean number of binary nucleon–nucleon (NN) collisions. This ratio is called the nuclear modification factor R_{AA}. In the absence of medium effects, one would expect $R_{AA} = 1$ for hard processes, which scale with the number of NN collisions. The R_{AA} for prompt and nonprompt J/ψ have been previously measured in PbPb at $\sqrt{s_{NN}} = 2.76$ TeV by CMS in bins of transverse momentum (p_T), rapidity (y) and collision centrality [22]. A strong centrality-dependent suppression has been observed for J/ψ with $p_T > 6.5$ GeV/c. The ALICE Collaboration has measured J/ψ down to $p_T = 0$ GeV/c in the electron channel at midrapidity ($|y| < 0.8$) [23] and in the muon channel at forward rapidity ($2.5 < y < 4$) [24]. Except for the most peripheral event selection, a suppression of inclusive J/ψ meson production is observed for all collision centralities. However, the suppression is smaller than that at $\sqrt{s_{NN}} = 0.2$ TeV [25], smaller at midrapidity than at forward rapidity, and, in the forward region, smaller for $p_T < 2$ GeV/c than

* e-mail: cms-publication-committee-chair@cern.ch

for $5 < p_T < 8\,\text{GeV/c}$ [26]. All these results were interpreted as evidence that the measured prompt J/ψ yield is the result of an interplay between (a) primordial production (J/ψ produced in the initial hard-scattering of the collisions), (b) colour screening and energy loss (J/ψ destroyed or modified by interactions with the surrounding medium), and (c) recombination/regeneration mechanisms in a deconfined partonic medium, or at the time of hadronization (J/ψ created when a free charm and a free anti-charm quark come close enough to each other to form a bound state) [27–29].

A complement to the R_{AA} measurement is the elliptic anisotropy coefficient v_2. This is the second Fourier coefficient in the expansion of the azimuthal angle (Φ) distribution of the J/ψ mesons, $dN/d\Phi \propto 1+2v_2\cos[2(\Phi-\Psi_{PP})]$ with respect to Ψ_{PP}, the azimuthal angle of the "participant plane" calculated for each event. In a noncentral heavy ion collision, the overlap region of the two colliding nuclei has a lenticular shape. The participant plane is defined by the beam direction and the direction of the shorter axis of the lenticular region. Typical sources for a nonzero elliptic anisotropy are a path length difference arising from energy loss of particles traversing the reaction zone, or different pressure gradients along the short and long axes. Both effects convert the initial spatial anisotropy into a momentum anisotropy v_2 [30]. The effect of energy loss is usually studied using high p_T and/or heavy particles (so-called "hard probes" of the medium), for which the parent parton is produced at an early stage of the collision. If the partons are emitted in the direction of the participant plane, they have on average a shorter in-medium path length than partons emitted orthogonally, leading to a smaller modification to their energy or, in the case of $Q\overline{Q}$ and the corresponding onium state, a smaller probability of being destroyed. Pressure gradients drive in-medium interactions that can modify the direction of the partons. This effect is most important at low p_T.

The v_2 of open charm (D mesons) and hidden charm (inclusive J/ψ mesons) was measured at the LHC by the ALICE Collaboration. The D mesons with $2 < p_T < 6\,\text{GeV/c}$ [31] were found to have a significant positive v_2, while for J/ψ mesons with $2 < p_T < 4\,\text{GeV/c}$ there was an indication of nonzero v_2 [32]. The precision of the results does not yet allow a determination of the origin of the observed anisotropy. One possible interpretation is that charm quarks at low p_T, despite their much larger mass than those of the u, s, d quarks, participate in the collective expansion of the medium. A second possibility is that there is no collective motion for the charm quarks, and the observed anisotropy is acquired via quark recombination [27,33,34].

In this paper, the R_{AA} and the v_2 for prompt and nonprompt J/ψ mesons are presented in several event centrality intervals and several kinematic regions. The results are based on event samples collected during the 2011 PbPb and 2013 pp LHC runs at a nucleon–nucleon centre-of-mass energy of 2.76 TeV, corresponding to integrated luminosities of $152\,\mu\text{b}^{-1}$ and $5.4\,\text{pb}^{-1}$, respectively.

2 Experimental setup and event selection

A detailed description of the CMS detector, together with a definition of the coordinate system and the relevant kinematic variables, can be found in Ref. [35]. The central feature of the CMS apparatus is a superconducting solenoid, of 6 m internal diameter and 15 m length. Within the field volume are the silicon tracker, the crystal electromagnetic calorimeter, and the brass and scintillator hadron calorimeter. The CMS apparatus also has extensive forward calorimetry, including two steel and quartz-fiber Cherenkov hadron forward (HF) calorimeters, which cover the range $2.9 < |\eta_{det}| < 5.2$, where η_{det} is measured from the geometrical centre of the CMS detector. The calorimeter cells, in the η-ϕ plane, form towers projecting radially outwards from close to the nominal interaction point. These detectors are used in the present analysis for the event selection, collision impact parameter determination, and measurement of the azimuthal angle of the participant plane.

Muons are detected in the pseudorapidity window $|\eta| < 2.4$, by gas-ionization detectors made of three technologies: drift tubes, cathode strip chambers, and resistive plate chambers, embedded in the steel flux-return yoke of the solenoid. The silicon tracker is composed of pixel detectors (three barrel layers and two forward disks on either side of the detector, made of 66 million $100 \times 150\,\mu\text{m}^2$ pixels) followed by microstrip detectors (ten barrel layers plus three inner disks and nine forward disks on either side of the detector, with strip pitch between 80 and 180 μm).

The measurements reported here are based on PbPb and pp events selected online (triggered) by a hardware-based dimuon trigger without an explicit muon momentum threshold (i.e. the actual threshold is determined by the detector acceptance and efficiency of the muon trigger). The same trigger logic was used during the pp and PbPb data taking periods.

In order to select a sample of purely inelastic hadronic PbPb (pp) collisions, the contributions from ultraperipheral collisions and noncollision beam background are removed offline, as described in Ref. [36]. Events are preselected if they contain a reconstructed primary vertex formed by at least two tracks and at least three (one in the case of pp events) HF towers on each side of the interaction point with an energy of at least 3 GeV deposited in each tower. To further suppress the beam-gas events, the distribution of hits in the pixel detector along the beam direction is required to be compatible with particles originating from the event vertex. These criteria select $(97 \pm 3)\%$ (>99%) of inelastic hadronic PbPb (pp) collisions with negligible contamination

from non-hadronic interactions [36]. Using this efficiency it is calculated that the PbPb sample corresponds to a number of minimum bias (MB) events $N_{\mathrm{MB}} = (1.16 \pm 0.04) \times 10^9$. The pp data set corresponds to an integrated luminosity of $5.4\,\mathrm{pb}^{-1}$ known to an accuracy of 3.7% from the uncertainty in the calibration based on a van der Meer scan [37]. The two data sets correspond to approximately the same number of elementary NN collisions.

Muons are reconstructed offline using tracks in the muon detectors ("standalone muons") that are then matched to tracks in the silicon tracker, using an algorithm optimized for the heavy ion environment [38]. In addition, an iterative track reconstruction algorithm [39] is applied to the PbPb data, limited to regions defined by the standalone muons. The pp reconstruction algorithm includes an iterative tracking step in the full silicon tracker. The final parameters of the muon trajectory are obtained from a global fit of the standalone muon with a matching track in the silicon tracker.

The centrality of heavy ion collisions, i.e. the geometrical overlap of the incoming nuclei, is correlated to the energy released in the collisions. In CMS, centrality is defined as percentiles of the distribution of the energy deposited in the HFs. Using a Glauber model calculation as described in Ref. [36], one can estimate variables related to the centrality, such as the mean number of nucleons participating in the collisions (N_{part}), the mean number of binary NN collisions (N_{coll}), and the average nuclear overlap function (T_{AA}) [40]. The latter is equal to the number of NN binary collisions divided by the NN cross section and can be interpreted as the NN-equivalent integrated luminosity per heavy ion collision, at a given centrality. In the following, N_{part} will be the variable used to show the centrality dependence of the measurements, while T_{AA} directly enters into the nuclear modification factor calculation. It should be noted that the PbPb hadronic cross section ($7.65 \pm 0.42\,\mathrm{b}$), computed with this Glauber simulation, results in an integrated luminosity of $152 \pm 9\,\mu\mathrm{b}^{-1}$, compatible within 1.2 sigma with the integrated luminosity based on the van der Meer scan, which has been evaluated to be $166 \pm 8\,\mu\mathrm{b}^{-1}$. All the R_{AA} results presented in the paper have been obtained using the N_{MB} event counting that is equivalent to $152\,\mu\mathrm{b}^{-1}$ expressed in terms of integrated luminosity.

Several Monte Carlo (MC) simulated event samples are used to model the signal shapes and evaluate reconstruction, trigger, and selection efficiencies. Samples of prompt and nonprompt J/ψ are generated with PYTHIA 6.424 [41] and decayed with EVTGEN 1.3.0 [42], while the final-state bremsstrahlung is simulated with PHOTOS 2.0 [43]. The prompt J/ψ is simulated unpolarized, a scenario in good agreement with pp measurements [44–46]. For nonprompt J/ψ, the results are reported for the polarization predicted by EVTGEN, roughly $\lambda_\theta = -0.4$, however not a well-defined value, since in many $\mathrm{B} \to \mathrm{J}/\psi X$ modes the spin alignment is either forced by angular momentum conservation or given as input from measured values of helicity amplitudes in decays. If the acceptances were different in pp and PbPb, they would not perfectly cancel in the R_{AA}. This would be the case if, for instance, some physics processes (such as polarization or energy loss) would affect the measurement in PbPb collisions with a strong kinematic dependence within an analysis bin. As in previous analyses [47–50], such possible physics effects are not considered as systematic uncertainties, but a quantitative estimate of this effect for two extreme polarization scenarios can be found in Ref. [22]. In the PbPb case, the PYTHIA signal events are further embedded in heavy ion events generated with HYDJET 1.8 [51], at the level of detector hits and with matching vertices. The detector response was simulated with GEANT4 [52], and the resulting information was processed through the full event reconstruction chain, including trigger emulation.

3 Analysis

Throughout this analysis the same methods for signal extraction and corrections are used for both the pp and PbPb data.

3.1 Corrections

For both R_{AA} and v_2 results, correction factors are applied event-by-event to each dimuon, to account for inefficiencies in the trigger, reconstruction, and selection of the $\mu^+\mu^-$ pairs. They were evaluated, using MC samples, in four dimensions (p_{T}, centrality, y, and L_{xyz}) for the PbPb results, and in three-dimensions (p_{T}, y, and L_{xyz}) for the pp results. After checking that the efficiencies on the prompt and nonprompt J/ψ MC samples near $L_{xyz} = 0$ are in agreement, two efficiency calculations are made. One calculation is made on the prompt J/ψ MC sample, as a function of p_{T}, in 10 rapidity intervals between $y = -2.4$ and $y = 2.4$, and 4 centrality bins (0–10%, 10–20%, 20–40%, and 40–100%). For each y and centrality interval, the p_{T} dependence of the efficiency is smoothed by fitting it with a Gaussian error function. A second efficiency is calculated using the nonprompt J/ψ MC sample, as a function of L_{xyz}, in the same y binning, but for coarser p_{T} bins and for centrality 0–100%. This is done in two steps. The efficiency is first calculated as a function of L^{true}_{xyz}, and then converted into an efficiency versus measured L_{xyz}, using a 2D dispersion map of L^{true}_{xyz} *vs.* L_{xyz}. In the end, each dimuon candidate selected in data, with transverse momentum p_{T}, rapidity y, centrality c, and $L_{xyz} = d\,(\mathrm{mm})$, is assigned an efficiency weight equal to

$$w = \mathrm{efficiency}^{\mathrm{prompt\,J}/\psi}(p_{\mathrm{T}}, y, c, L_{xyz} = 0) \times \frac{\mathrm{efficiency}^{\mathrm{nonprompt\,J}/\psi}(p_{\mathrm{T}}, y, L_{xyz} = d)}{\mathrm{efficiency}^{\mathrm{nonprompt\,J}/\psi}(p_{\mathrm{T}}, y, L_{xyz} = 0)}. \quad (1)$$

The individual components of the MC efficiency (tracking reconstruction, standalone muon reconstruction, global muon fit, muon identification and selection, triggering) are cross-checked using single muons from J/ψ decays in simulated and collision data, with the *tag-and-probe* technique (T&P) [53]. For all but the tracking reconstruction, scaling factors (calculated as the ratios between the data and MC T&P obtained efficiencies), estimated as a function of the muon p_T in several muon pseudorapidity regions, are used to scale the dimuon MC-calculated efficiencies. They are applied event-by-event, as a weight, to each muon that passes all analysis selections and enter the mass and $\ell_{J/\psi}$ distributions. The weights are similar for the pp and PbPb samples, and range from 1.02 to 0.6 for single muons with $p_T > 4 - 5\,\text{GeV/c}$ and $p_T < 3.5\,\text{GeV/c}$, respectively. For the tracking efficiency, which is above 99% even in the case of PbPb events, the full difference between data and MC T&P results (integrated over all the kinematic region probed) is propagated as a global (common to all points) systematic uncertainty.

3.2 Signal extraction

The single-muon acceptance and identification criteria are the same as in Ref. [22]. Opposite-charge muon pairs, with invariant mass between 2.6 and 3.5 GeV/c^2, are fitted with a common vertex constraint and are kept if the fit χ^2 probability is larger than 1%. Results are presented in up to six bins of absolute J/ψ meson rapidity (equally spaced between 0 and 2.4) integrated over p_T ($6.5 < p_T < 30$ GeV/c), up to six bins in p_T ([6.5, 8.5], [8.5, 9.5], [9.5, 11], [11, 13], [13, 16], [16, 30] GeV/c) integrated over rapidity ($|y| < 2.4$), and up to three additional low-p_T bins ([3, 4.5], [4.5, 5.5], [5.5, 6.5] GeV/c) at forward rapidity ($1.6 < |y| < 2.4$). The lower p_T limit for which the results are reported is imposed by the detector acceptance, the muon reconstruction algorithm, and the selection criteria used in the analysis. The PbPb sample is split in bins of collision centrality, defined using fractions of the inelastic hadronic cross section where 0% denotes the most central collisions. This fraction is determined from the HF energy distribution [54]. The most central (highest HF energy deposit) and most peripheral (lowest HF energy deposit) centrality bins used in the analysis are 0–5% and 60–100%, and 0–10% and 50–100%, for prompt and nonprompt J/ψ results, respectively. The rest of the centrality bins are in increments of 5% up to 50% for the high p_T prompt J/ψ results integrated over y, and in increments of 10% for all other cases. The N_{part} values, computed for events with a flat centrality distribution, range from 381 ± 2 in the 0–5% bin to 14 ± 2 in the 60–100% bin. If the events would be distributed according to the number of NN collisions, N_{coll}, which is expected for initially produced hard probes, the average N_{part} would become 25 instead of 14 for the most peripheral bin, and 41 instead of 22 in the case of the 50–100% bin. For the other finer bins, the difference is negligible (less than 3%).

The same method for signal extraction is used in both the v_2 and the R_{AA} analyses, for both the PbPb and pp samples. The separation of prompt J/ψ mesons from those coming from b hadron decays relies on the measurement of a secondary $\mu^+\mu^-$ vertex displaced from the primary collision vertex. The displacement $\vec{r}$ between the $\mu^+\mu^-$ vertex and the primary vertex is measured first. Then, the most probable decay length of b hadron in the laboratory frame [55] is calculated as

$$L_{xyz} = \frac{\hat{u}^T S^{-1} \vec{r}}{\hat{u}^T S^{-1} \hat{u}}, \tag{2}$$

where $\hat{u}$ is the unit vector in the direction of the J/ψ meson momentum ($\vec{p}$) and S is the sum of the primary and secondary vertex covariance matrices. From this quantity, the pseudo-proper decay length $\ell_{J/\psi} = L_{xyz}\, m_{J/\psi}/p$ (which is the decay length of the J/ψ meson) is computed as an estimate of the b hadron decay length.

To measure the fraction of the J/ψ mesons coming from b hadron decays (the so-called *b fraction*), the invariant-mass spectrum of $\mu^+\mu^-$ pairs and their $\ell_{J/\psi}$ distribution are fitted sequentially in an extended unbinned maximum likelihood fit. The fits are performed for each p_T, $|y|$, and centrality bin of the analysis, and in addition in the case of the PbPb v_2 analysis, in four bins in $|\Delta\phi| = |\phi - \Psi_2|$, equally spaced between 0 and $\pi/2$. The second-order "event plane" angle Ψ_2, measured as explained below, corresponds to the event-by-event azimuthal angle of maximum particle density. It is an approximation of the participant plane angle Ψ_{PP}, which is not directly observable.

The fitting procedure is similar to the one used in earlier analyses of pp collisions at $\sqrt{s} = 7$ TeV [56], and PbPb collisions at $\sqrt{s_{NN}} = 2.76$ TeV [22]. The J/ψ meson mass distribution is modelled by the sum of a Gaussian function and a Crystal Ball (CB) function [57], with a common mean m_0 and independent widths. The CB radiative tail parameters are fixed to the values obtained in fits to simulated distributions for different kinematic regions [50]. The invariant mass background probability density function (PDF) is an exponential function whose parameters are allowed to float in each fit. Since the mass resolution depends on y and p_T, all resolution-related parameters are left free when binning as a function of $|y|$ or p_T. In the case of centrality binning, the width of the CB function is left free, while the rest of the parameters are fixed to the centrality-integrated results, 0–100%, for a given p_T and $|y|$ bin. When binning in $|\Delta\phi|$, all signal parameters are fixed to their values in the $|\Delta\phi|$-integrated fit.

The $\ell_{J/\psi}$ distribution is modeled by a prompt signal component represented by a resolution function, a nonprompt component given by an exponential function convoluted with the resolution function, and the continuum background component represented by the sum of the resolution function plus three exponential decay functions to take into account long-lived background components [56]. The resolution function is comprised of the sum of two Gaussian functions, which depend upon the per-event uncertainty of the measured $\ell_{J/\psi}$, determined from the covariance matrices of the primary and secondary vertex fits. The fit parameters of the $\ell_{J/\psi}$ distribution were determined through a series of fits. Pseudo-proper decay length background function parameters are fixed using dimuon events in data located on each side of the J/ψ resonance peak. In all cases, the b fraction is a free fit parameter. An example of 2D fits is given in Fig. 1.

The v_2 analysis follows closely the event plane method described in Ref. [58]. The J/ψ mesons reconstructed with $y > 0$ ($y < 0$) are correlated with the event plane Ψ_2 found using energy deposited in a region of the HF spanning $-5 < \eta < -3$ ($3 < \eta < 5$). This is chosen to introduce a rapidity gap between the particles used in the event plane determination and the J/ψ meson, in order to reduce the effect of other correlations that might exist, such as those from dijet production. To account for nonuniformities in the detector acceptance that can lead to artificial asymmetries in the event plane angle distribution and thereby affect the deduced v_2 values, a Fourier analysis "flattening" procedure [59] is used, where each calculated event plane angle is shifted slightly to recover a uniform azimuthal distribution, as described in Ref. [58]. The event plane has a resolution that depends on centrality, and is caused by the finite number of particles used in its determination.

The corrections applied event-by-event ensure that the prompt and nonprompt yields extracted from fitting the invariant mass and $\ell_{J/\psi}$ distributions account for reconstruction and selection inefficiencies. As such, after extracting the yields in each $|y|$, p_T, centrality (and $|\Delta\phi|$) bin, the v_2 and R_{AA} can be calculated directly. The R_{AA} is defined by

$$R_{AA} = \frac{N^{J/\psi}_{PbPb}}{(T_{AA}\,\sigma^{J/\psi}_{pp})}, \tag{3}$$

where $N^{J/\psi}_{PbPb}$ is the number of prompt or nonprompt J/ψ mesons produced per PbPb collision, $\sigma^{J/\psi}_{pp}$ is the corresponding pp cross section, and T_{AA} is the nuclear overlap function.

The v_2 is calculated by fitting the $[1/N^{J/\psi}_{total}][dN^{J/\psi}/d|\Delta\Phi|]$ distributions with the function $1+2v_2^{obs}\cos(|2\Delta\phi|)$, where the $N^{J/\psi}_{total}$ is the prompt or nonprompt J/ψ yield integrated over azimuth for each kinematic bin. An example of such a fit is shown in Fig. 2. The final v_2 coefficient in the event plane method is evaluated by dividing the observed

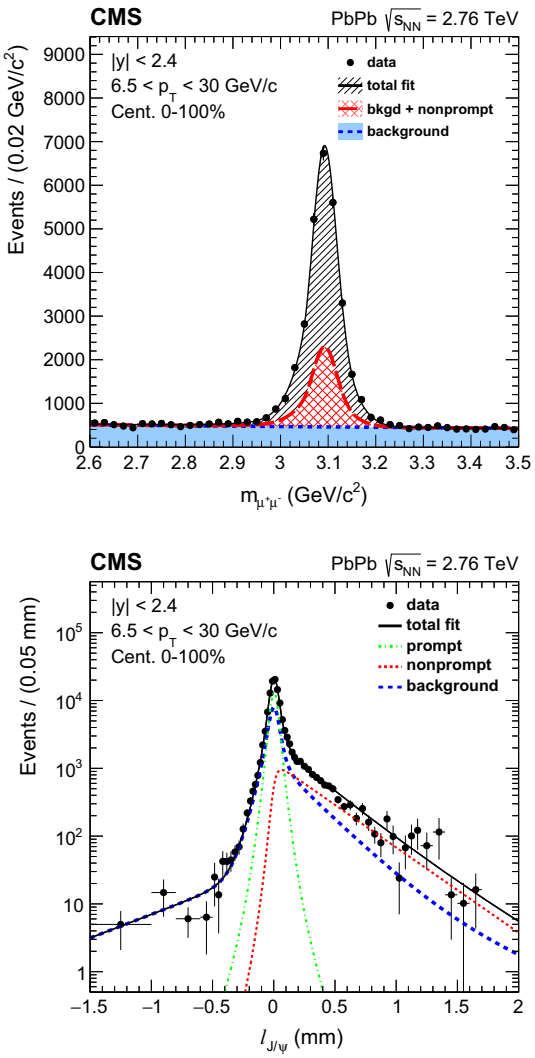

Fig. 1 Invariant mass spectra (*top*) and pseudo-proper decay length distribution (*bottom*) of $\mu^+\mu^-$ pairs in centrality 0–100% and integrated over the rapidity range $|y| < 2.4$ and the p_T range $6.5 < p_T < 30$ GeV/c. The *error bars* on each point represent statistical uncertainties. The projections of the two-dimensional fit onto the respective axes are overlaid as *solid black lines*. The *dashed green* and *red lines* show the fitted contribution of prompt and nonprompt J/ψ. The fitted background contributions are shown as *dotted blue lines*

value v_2^{obs} by an event-averaged resolution-correction R, i.e. $v_2 = v_2^{obs}/R$, as described in Ref. [60]. The factor R, calculated experimentally as described in Ref. [58], can range from 0 to 1, with a better resolution corresponding to a larger value of R. No difference is observed when determining R using the dimuon-triggered events analysed here, compared to the values used in Ref. [58] for the analysis of charged hadrons. For this paper, the v_2 analysis is restricted to the centrality interval 10–60% to ensure a nonsymmetric overlap region in the colliding nuclei, while maintaining a good event plane resolution ($R \gtrsim 0.8$ in the event centrality ranges

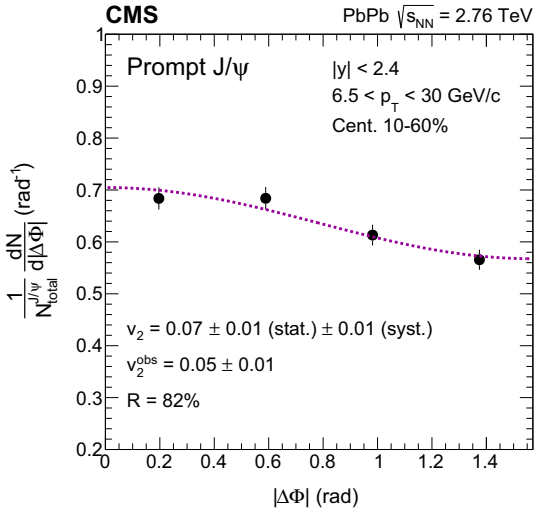

Fig. 2 The $|\Delta\Phi|$ distribution of high p_T prompt J/ψ mesons, $6.5 < p_T < 30\,\text{GeV/c}$, measured in the rapidity range $|y| < 2.4$ and event centrality 10–60%, normalized by the bin width and the sum of the prompt yields in all four $\Delta\Phi$ bins. The *dashed line* represents the function $1 + 2v_2^{obs}\cos(|2\Delta\Phi|)$ used to extract the v_2^{obs}. The event-averaged resolution correction factor, corresponding to this event centrality, is also listed, together with the calculated final v_2 for this kinematic bin. The systematic uncertainty listed in the legend includes the 2.7% global uncertainty from the event plane measurement

in which results are reported: 10–20%, 20–30%, and 30–60%).

3.3 Estimation of uncertainties

Several sources of systematic uncertainties are considered for both R_{AA} and v_2 analyses. They are mostly common, thus calculated and propagated in a similar way.

The systematic uncertainties in the signal extraction method (fitting) are evaluated by varying the analytical form of each component of the PDF hypotheses. For the invariant mass PDF, as an alternative signal shape, a sum of two Gaussian functions is used, with shared mean and both widths as free parameters in the fit. For the same PDF, the uncertainty in the background shape is evaluated using a first order Chebychev polynomial. For the differential centrality bins, with the invariant mass signal PDF parameters fixed to the 0–100% bin, an uncertainty is calculated by performing fits in which the constrained parameters are allowed to vary with a Gaussian PDF. The mean of the constraining Gaussian function and the initial value of the constrained parameters come from the fitting in the 0–100% bin with no fixed parameters. The uncertainties of the parameters in the 0–100% bin is used as a width of the constraining Gaussian. For the lifetime PDF components, the settings that could potentially affect the b fraction are changed. The $\ell_{J/\psi}$ shape of the nonprompt J/ψ is taken directly from the reconstructed one in simulation and converted to a PDF. Tails of this PDF, where the MC statistics are insufficient, are mirrored from neighboring points, weighted with the corresponding efficiency. The sum in quadrature of all yield variations with respect to the nominal fit is propagated in the calculation of the systematic uncertainty in the final results. The variations across all R_{AA} (v_2) analysis bins are between 0.7 and 16% (2.6 and 38%) for prompt J/ψ, and 1.4 and 19% (20 and 81%) for nonprompt J/ψ. They increase from mid to forward rapidity, from high- to low-p_T, and for PbPb results also from central to peripheral bins.

Three independent uncertainties are assigned for the dimuon efficiency corrections. One addresses the uncertainty on the parametrization of the efficiency *vs.* p_T, y, and centrality. For the R_{AA} results, it is estimated, in each signal y and centrality bin, by randomly moving 100 times, each individual efficiency versus p_T point within its statistical uncertainty, re-fitting with the Gaussian error function, and recalculating each time a corrected MC signal yield. For the v_2 results, this procedure is not practical: it requires reweighting and re-fitting many times the full data sample. So in this case, the uncertainty is estimated by changing two settings in the nominal efficiency, and re-fitting data only once, with the modified efficiency: (a) using binned efficiency instead of fits, and (b) using only the nonprompt J/ψ MC sample, integrated over all event centralities. The relative uncertainties for this source, propagated into the final results, are calculated for R_{AA} as the root-mean-square of the 100 yield variations with respect to the yield obtained with the nominal efficiency parametrization, and for the v_2 analysis as the full difference between the nominal and the modified-efficiency results. Across all R_{AA} (v_2) analysis bins, the values are between 0.6 and 20% (1.5 and 54%) for prompt J/ψ, and 0.7 and 24% (6.1 and 50%) for nonprompt J/ψ results. These uncertainties increase from high to low p_T, and from mid to forward rapidity but do not have a strong centrality dependence.

A second uncertainty addresses the accuracy of the efficiency *vs.* L_{xyz} calculation, and is estimated by changing the L_{xyz} resolution. It is done in several steps: (a) the binning in the L^{true}_{xyz} *vs.* L_{xyz} maps is changed; (b) the dimuon efficiency weights are recalculated; c) the data is reweighed and refitted to extract the signal yields. The variations across all R_{AA} (v_2) analysis bins are between 0.025 and 3.7% (0.1 and 16%) for prompt J/ψ, and 0.1 and 13% (29 and 32%) for nonprompt J/ψ results. In the case of the prompt J/ψ, the variations are small and rather constant across all bins, around 2-3%, with the 16% variation being reached only in the lowest-p_T bin in the v_2 analysis. For nonprompt J/ψ the variations increase from mid to forward rapidity, and for PbPb also from peripheral to central bins.

Finally, a third class of uncertainty arises from the scaling factors. For the v_2 analysis, the full difference between results with and without T&P corrections is propagated to the final systematic uncertainty. It varies between 0.4 and

7.4% for prompt J/ψ, and 5.4 and 8.8% for nonprompt J/ψ results. For the R_{AA} analysis, this uncertainty comprises two contributions. A parametrization uncertainty was estimated by randomly moving each of the data T&P efficiency points within their statistical uncertainty, recalculating each time the scaling factors and the dimuon efficiencies in all the analysis bins, and propagating the root-mean-square of all variations to the total T&P uncertainty. In addition, a systematic uncertainty was estimated by changing different settings of the T&P method. The contributions are similar for the prompt and nonprompt J/ψ results, and vary between 1.4 and 13% across all bins, for the combined trigger, identification, and reconstruction efficiencies, with the largest uncertainties in the forward and low p_T regions. On top of these bin-by-bin T&P uncertainties, an uncertainty in the tracking reconstruction efficiency, 0.3 and 0.6% for each muon track, for pp and PbPb, respectively, is doubled for dimuon candidates, and considered as a global uncertainty in the final results.

There is one additional source of uncertainty that is particular to each analysis. For the R_{AA} results, it is the T_{AA} uncertainty, which varies between 16 and 4.1% from most peripheral (70–100%) to most central (0–5%) events, and it has a value of 5.6% for the 0–100% case, estimated as described in Ref. [36]. For the v_2 analysis, uncertainties are assigned for the event plane measurement. A systematic uncertainty is associated with the event plane flattening procedure and the resolution correction determination (± 1% [60]), and another with the sensitivity of the measured v_2 values to the size of the minimum η gap (2.5%, following Ref. [60]). The two uncertainties are added quadratically to a total of 2.7% global uncertainty in the v_2 measurement.

The total systematic uncertainty in the R_{AA} is estimated by summing in quadrature the uncertainties from the signal extraction and efficiency weighting. The range of the final uncertainties on prompt and nonprompt J/ψ R_{AA} is between 2.1 and 22%, and 2.8 and 28%, respectively, across bins of the analysis. The uncertainty in the integrated luminosity of the pp data (3.7%), N_{MB} events in PbPb data (3%), and tracking efficiency (0.6% for pp and 1.2% for PbPb data) are considered as global uncertainties.

The total systematic uncertainty for v_2 is estimated by summing in quadrature the contributions from the yield extraction and efficiency corrections. The range of the final uncertainties on prompt and nonprompt J/ψ v_2 results is between 10 and 57%, and 37 and 100%, respectively.

3.4 Displaying uncertainties

In all the results shown, statistical uncertainties are represented by error bars, and systematic uncertainties by boxes centered on the points. For the v_2 results, the global uncertainty from the event plane measurement is not included in the point-by-point uncertainties. Boxes plotted at $R_{AA} = 1$ represent the scale of the global uncertainties. For R_{AA} results plotted as a function of p_T or $|y|$, the statistical and systematic uncertainties include the statistical and systematic components from both PbPb and pp samples, added in quadrature. For these types of results, the systematic uncertainty on T_{AA}, the pp sample integrated luminosity uncertainty, the uncertainty in the N_{MB} of PbPb events, and the tracking efficiency are added in quadrature and shown as a global uncertainty.

For R_{AA} results shown as a function of N_{part}, the uncertainties on T_{AA} are included in the systematic uncertainty, point-by-point. The global uncertainty plotted at $R_{AA} = 1$ as a grey box includes in this case the statistical and systematic uncertainties from the pp measurement, the integrated luminosity uncertainty for the pp data, the uncertainty in the N_{MB} of PbPb events, and the tracking efficiency uncertainty, added in quadrature. When showing R_{AA} *vs.* N_{part} separately for different p_T or $|y|$ intervals, the statistical and systematic uncertainties from the pp measurement are added together in quadrature and plotted as a coloured box at $R_{AA} = 1$. In addition, a second global uncertainty, that is common for all the p_T and $|y|$ bins, is calculated as the quadratic sum of the integrated luminosity uncertainty for pp data, the uncertainty in N_{MB} of PbPb events, and the tracking efficiency uncertainty, and is plotted as an empty box at $R_{AA} = 1$.

4 Results

For all results plotted versus p_T or $|y|$, the abscissae of the points correspond to the centre of the respective bin, and the horizontal error bars reflect the width of the bin. When plotted as a function of centrality, the abscissae are average N_{part} values corresponding to events flatly distributed across centrality. For the R_{AA} results, the numerical values of the numerator and denominator of Eq. (3) are available in tabulated form in Appendix A.

4.1 Prompt J/ψ

The measured prompt J/ψ v_2, for 10–60% event centrality and integrated over $6.5 < p_T < 30$ GeV/c and $|y| < 2.4$, is $0.066 \pm 0.014\,(\text{stat}) \pm 0.014\,(\text{syst}) \pm 0.002\,(\text{global})$. The significance corresponding to a deviation from a $v_2 = 0$ value is 3.3 sigma. Figure 3 shows the dependence of v_2 on centrality, $|y|$, and p_T. For each of these results, the dependence on one variable is studied by integrating over the other two. A nonzero v_2 value is measured in all the kinematic bins studied. The observed anisotropy shows no strong centrality, rapidity, or p_T dependence.

In Fig. 4, the R_{AA} of prompt J/ψ as a function of centrality, $|y|$, and p_T are shown, integrating in each case over the other two variables. The R_{AA} is suppressed even for the most peripheral bin (60–100%), with the suppression slowly

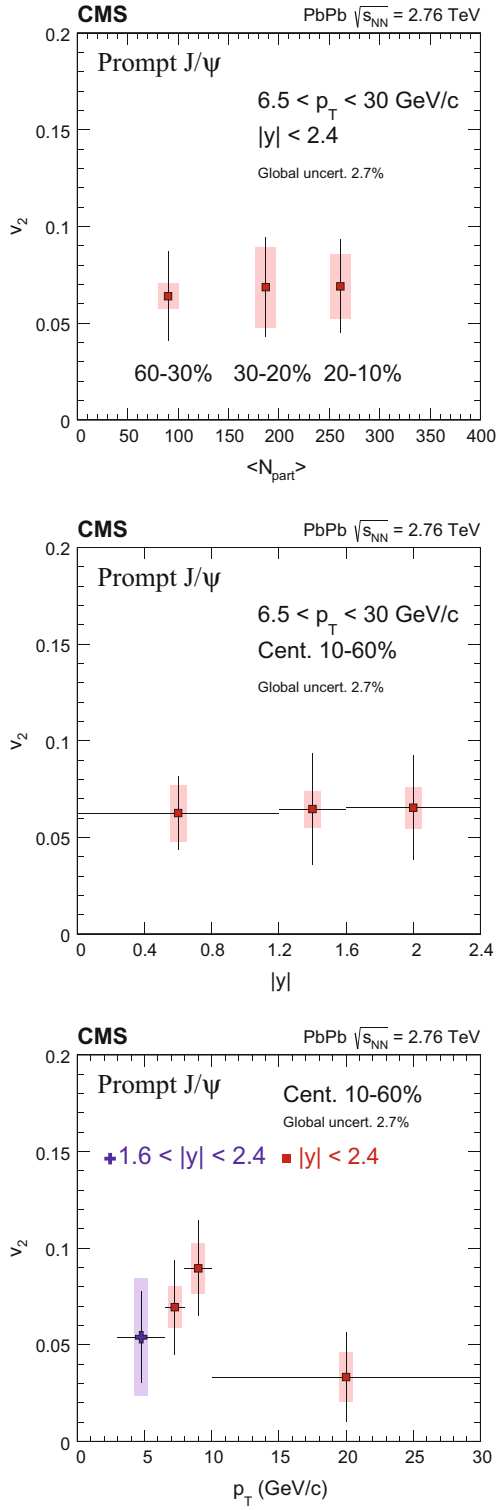

Fig. 3 Prompt J/ψ v_2 as a function of centrality (*top*), rapidity (*middle*), and p_T (*bottom*). The *bars* (*boxes*) represent statistical (systematic) point-by-point uncertainties. The global uncertainty, listed in the legend, is not included in the point-by-point uncertainties. *Horizontal bars* indicate the bin width. The average N_{part} values correspond to events flatly distributed across centrality

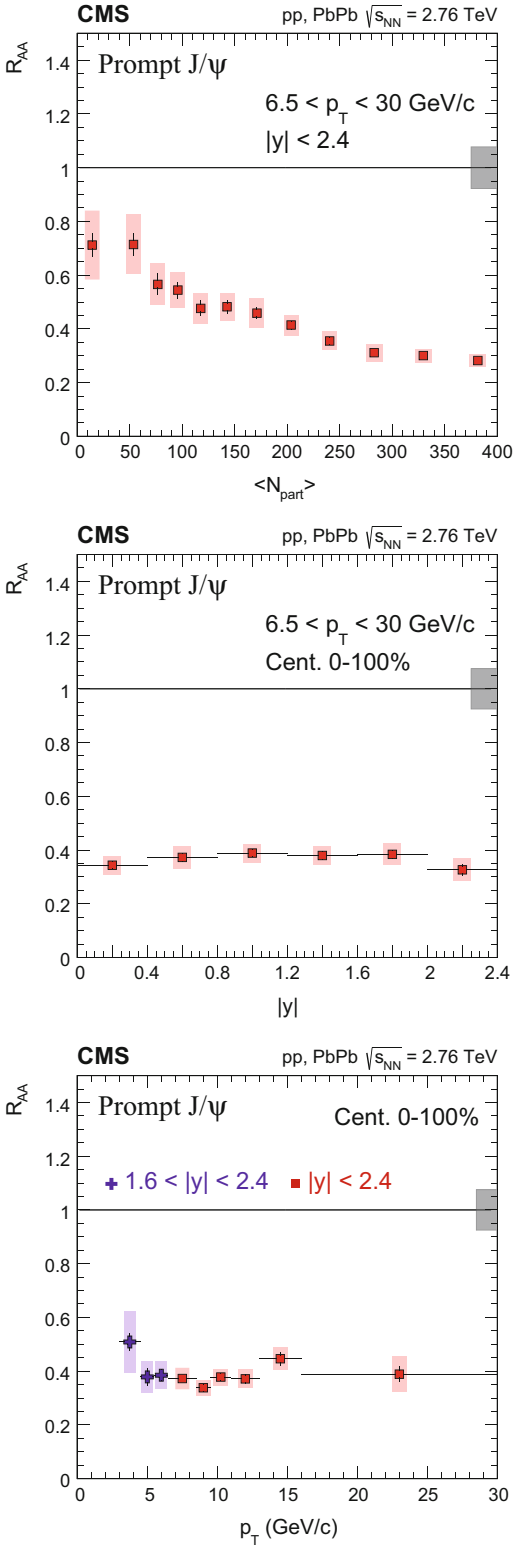

Fig. 4 Prompt J/ψ R_{AA} as a function of centrality (*top*), rapidity (*middle*), and p_T (*bottom*). The *bars* (*boxes*) represent statistical (systematic) point-by-point uncertainties. The *gray boxes* plotted on the right side at $R_{AA} = 1$ represent the scale of the global uncertainties. The average N_{part} values correspond to events flatly distributed across centrality

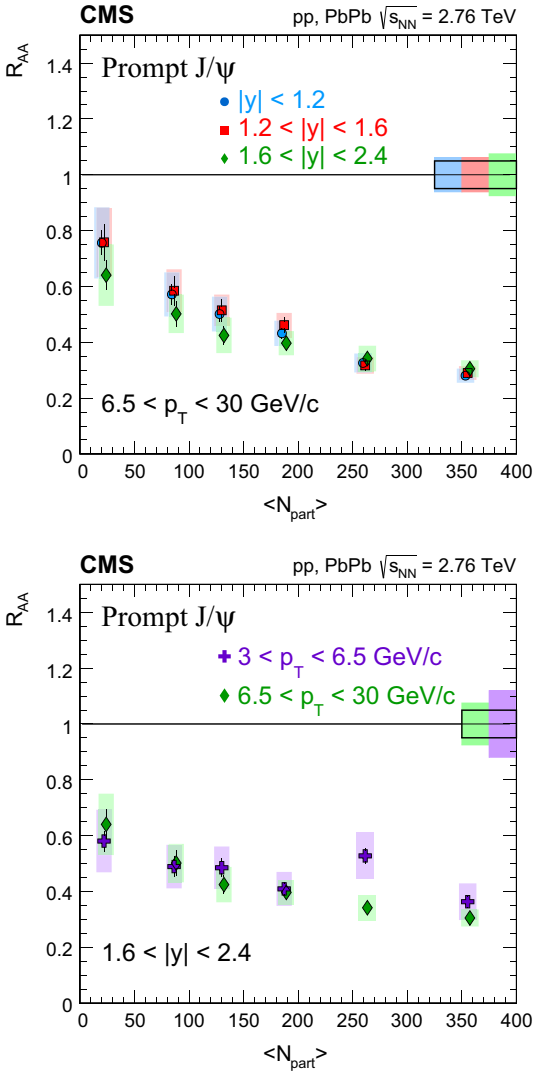

Fig. 5 *Top* Prompt J/ψ R_{AA} as a function of centrality at high p_{T}, $6.5 < p_{\mathrm{T}} < 30\,\mathrm{GeV/c}$, for three different $|y|$ regions. The high-p_{T} mid- and forward-rapidity points are shifted horizontally by $\Delta N_{\mathrm{part}} = 2$ for better visibility. *Bottom* Prompt J/ψ R_{AA} as a function of centrality, at forward rapidity, $1.6 < |y| < 2.4$, for two different p_{T} regions. The *bars* (*boxes*) represent statistical (systematic) point-by-point uncertainties. The *boxes* plotted on the right side at $R_{\mathrm{AA}} = 1$ represent the scale of the global uncertainties: the *coloured boxes* show the statistical and systematic uncertainties from pp measurement, and the *open box* shows the global uncertainties common to all data points. The average N_{part} values correspond to events flatly distributed across centrality

increasing with N_{part}. The R_{AA} for the most central events (0–5%) is measured for $6.5 < p_{\mathrm{T}} < 30\,\mathrm{GeV/c}$ and $|y| < 2.4$ to be $0.282 \pm 0.010\,(\mathrm{stat}) \pm 0.023\,(\mathrm{syst})$. No strong rapidity or p_{T} dependence of the suppression is observed.

Two double-differential studies are also made, in which a simultaneous binning in centrality and $|y|$, or in centrality and p_{T} is done. Figure 5 (*top*) shows the centrality dependence of high p_{T} ($6.5 < p_{\mathrm{T}} < 30\,\mathrm{GeV/c}$) prompt J/$\psi$ R_{AA} measured in three $|y|$ intervals. A similar suppression pattern is observed for all rapidities. Figure 5 (*bottom*) shows,

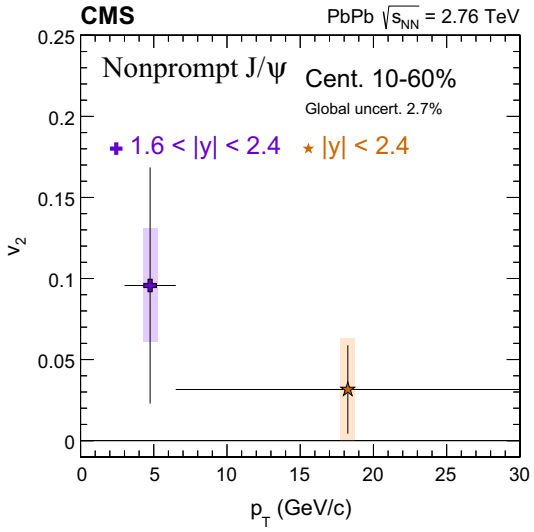

Fig. 6 Nonprompt J/ψ v_2 as a function of p_{T}. The *bars* (*boxes*) represent statistical (systematic) point-by-point uncertainties. The global uncertainty, listed in the legend, is not included in the point-by-point uncertainties. *Horizontal bars* indicate the bin width

for $1.6 < |y| < 2.4$, the p_{T} dependence of R_{AA} *vs.* N_{part}. The suppression at low p_{T} ($3 < p_{\mathrm{T}} < 6.5\,\mathrm{GeV/c}$) is consistent with that at high p_{T} ($6.5 < p_{\mathrm{T}} < 30\,\mathrm{GeV/c}$).

4.2 Nonprompt J/ψ

Figure 6 shows the nonprompt J/ψ v_2 *vs.* p_{T} for 10–60% event centrality, in two kinematic regions: $6.5 < p_{\mathrm{T}} < 30\,\mathrm{GeV/c}$ and $|y| < 2.4$, and $3 < p_{\mathrm{T}} < 6.5\,\mathrm{GeV/c}$ and $1.6 < |y| < 2.4$. The measured v_2 for the high-(low-) p_{T} is $0.032 \pm 0.027\,(\mathrm{stat}) \pm 0.032\,(\mathrm{syst}) \pm 0.001\,(\mathrm{global})$ ($0.096 \pm 0.073\,(\mathrm{stat}) \pm 0.035\,(\mathrm{syst}) \pm 0.003\,(\mathrm{global})$). This is obtained from the fit to the $|\Delta\Phi|$ distribution (as described in Sect. 3.2) with a χ^2 probability of 22(20)%. Fitting the same distribution with a constant (corresponding to the $v_2 = 0$ case) the χ^2 probability is 11(8)%. Both measurements are consistent with each other and with a v_2 value of zero, though both nominal values are positive.

In Fig. 7, the R_{AA} of nonprompt J/ψ as a function of centrality, $|y|$, and p_{T} are shown, integrating in each case over the other two variables. A steady increase of the suppression is observed with increasing centrality of the collision. The R_{AA} for the most central events (0–10%) measured for $6.5 < p_{\mathrm{T}} < 30\,\mathrm{GeV/c}$ and $|y| < 2.4$ is $0.332 \pm 0.017\,(\mathrm{stat}) \pm 0.028\,(\mathrm{syst})$. Stronger suppression is observed with both increasing rapidity and p_{T}.

As for the prompt production case, two double-differential studies were done, simultaneously binning in centrality and $|y|$ or p_{T}. Figure 8 (*top*) shows the rapidity dependence of R_{AA} *vs.* N_{part} for high p_{T} nonprompt J/ψ. Figure 8 (*bottom*) shows, for $1.6 < |y| < 2.4$, the p_{T} dependence of R_{AA} *vs.* N_{part}. The centrality dependences of the three $|y|$ intervals

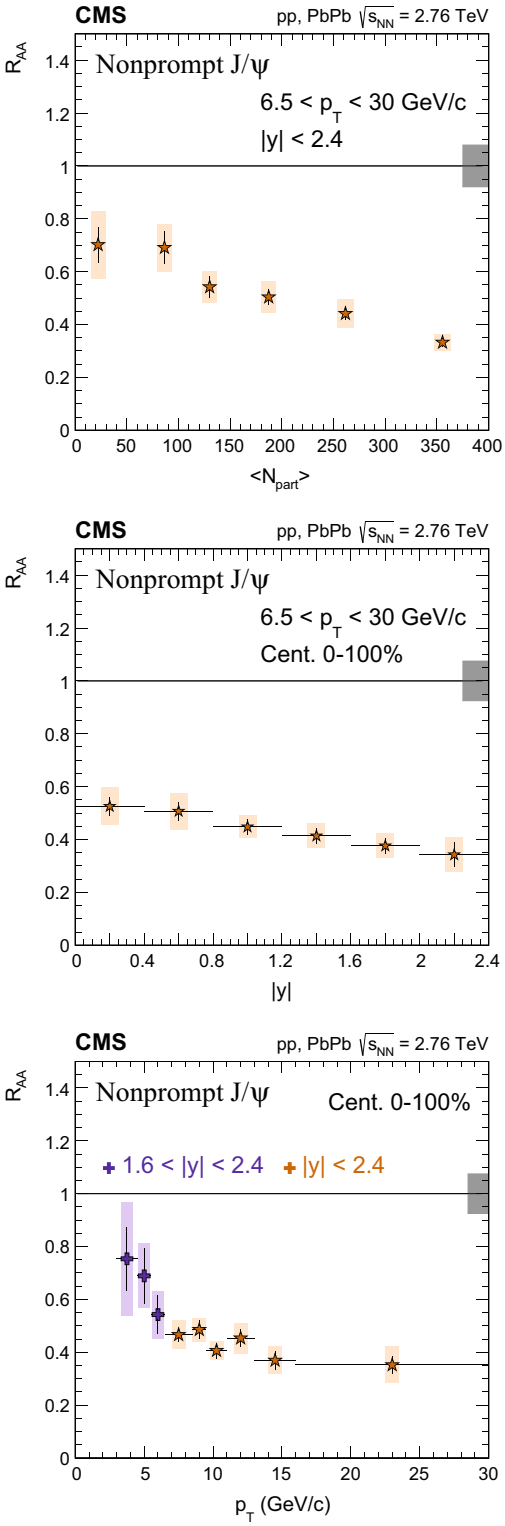

Fig. 7 Nonprompt J/ψ R_{AA} as a function of centrality (*top*), rapidity (*middle*), and p_T (*bottom*). The *bars* (*boxes*) represent statistical (systematic) point-by-point uncertainties. The *gray boxes* plotted on the right side at $R_{AA} = 1$ represent the scale of the global uncertainties. For R_{AA} *vs.* N_{part}, the average N_{part} values correspond to events flatly distributed across centrality

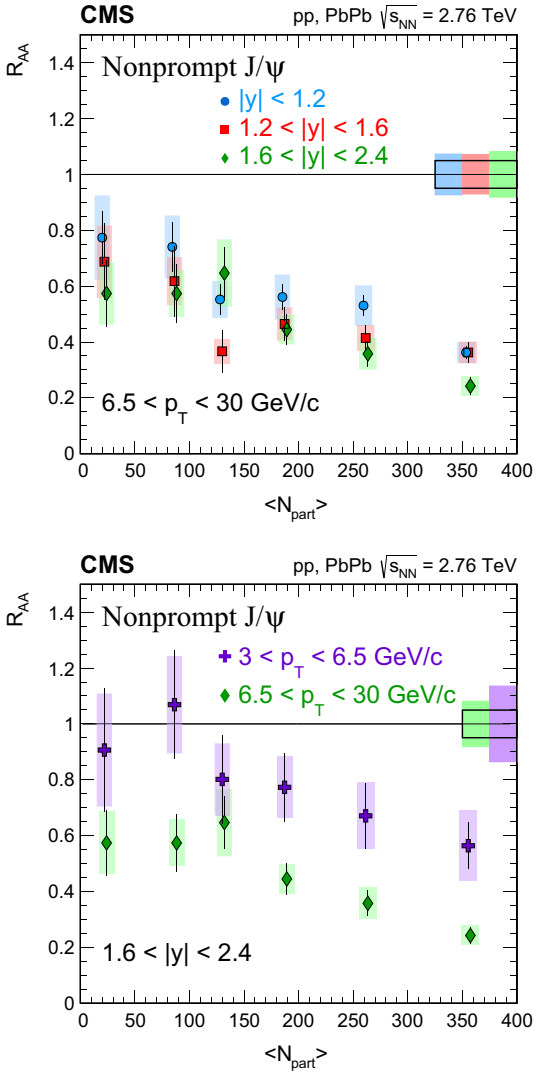

Fig. 8 *Top* Nonprompt J/ψ R_{AA} as a function of centrality at high p_T, 6.5 < p_T < 30 GeV/c, for three different $|y|$ regions. The high-p_T mid- and forward-rapidity points are shifted horizontally by $\Delta N_{part} = 2$ for better visibility. *Bottom* Nonprompt J/ψ R_{AA} as a function of centrality, at forward rapidity, 1.6 < $|y|$ < 2.4, for two different p_T regions. The *bars* (*boxes*) represent statistical (systematic) point-by-point uncertainties. The *boxes* plotted on the right side at $R_{AA} = 1$ represent the scale of the global uncertainties: the *coloured boxes* show the statistical and systematic uncertainties from pp measurement, and the *open box* shows the global uncertainties common to all data points. The average N_{part} values correspond to events flatly distributed across centrality

are quite similar, and the same is true for the two p_T ranges. As was also seen in Fig. 7, smaller suppression is observed at lower $|y|$ and lower p_T.

5 Discussion

In this section, the R_{AA} and v_2 results are compared first for open and hidden charm, and then for open charm and

beauty, using data from the ALICE experiment [31,61,62]. For open charm, the measurements of R_{AA} *vs.* N_{part} of prompt D^0 mesons, and of averaged prompt D mesons (D^0, D^+ and D^{*+} combined), measured in $|y| < 0.5$ at low p_T ($2 < p_T < 5\,GeV/c$), and high p_T ($6 < p_T < 12\,GeV/c$) [61] are used. These are compared to hidden charm data from the prompt J/ψ results described in this paper, in two p_T regions that are similar to the D measurement, i.e. ($3 < p_T < 6.5\,GeV/c$, $1.6 < |y| < 2.4$) and ($6.5 < p_T < 30\,GeV/c$, $|y| < 1.2$). For the R_{AA} comparison of open charm *vs.* beauty, the averaged prompt D mesons measured in $|y| < 0.5$ [62] are compared to the nonprompt J/ψ results reported in this paper for $|y| < 1.2$. The p_T interval ($8 < p_T < 16\,GeV/c$) for the D is chosen to correspond to that of the parent B mesons of the CMS nonprompt J/ψ result [62].

For the v_2 results, the p_T dependence reported in this paper for both prompt and nonprompt J/ψ in the centrality 10–60% bin are compared with the v_2 of the averaged D mesons [31] measured in the 30–50% centrality bin. In addition, the CMS charged-hadron v_2 results, measured for $|\eta| < 0.5$, derived for 10–60% centrality bin from Refs. [60] and [58], are added to the comparison.

5.1 Open versus hidden charm

The top two panels of Fig. 9 show the R_{AA} dependence on the centrality of the prompt J/ψ (bound $Q\overline{Q}$ state) and of prompt D (charm-light states $Q\overline{q}$) mesons, for low- (*top*) and high- (*middle*) p_T selections. In both cases, the mesons suffer a similar suppression, over the whole N_{part} range, even though the charmonium yield should be affected by colour screening [4,48], potentially by final-state nuclear interactions unrelated to the QGP [63–67], and by rather large feed-down contributions from excited states [68,69]. Moreover, common processes (i.e. recombination or energy loss effects) are expected to affect differently the open and hidden charm [26,27,70,71]. While the present results cannot resolve all these effects, the comparison of open and hidden charm could help to determine their admixture.

A comparison of the p_T dependence of the azimuthal anisotropy v_2 between the prompt J/ψ and D mesons is made in the bottom panel of Fig. 9. While the R_{AA} is similar both at low and high p_T, the v_2 of prompt J/ψ at low p_T is lower than that of both D mesons and charged hadrons. At high p_T, all three results, within the uncertainties, are similar: the prompt J/ψ results seem to point to a similar anisotropy as the light-quarks hadrons, hinting at a flavour independence of the energy-loss path-length dependence. The prompt J/ψ results could help advance the theoretical knowledge on the relative contribution of the regenerated charmonium yield, as this is the only type of J/ψ expected to be affected by the collective expansion of the medium. Such prompt J/ψ

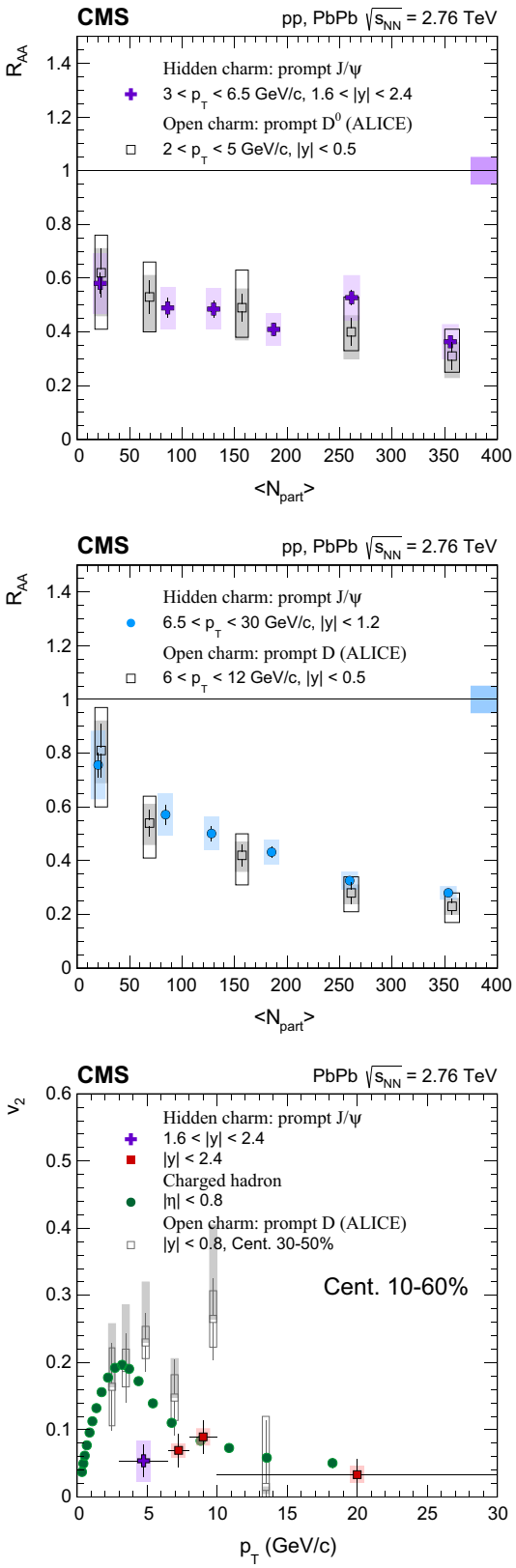

Fig. 9 Prompt J/ψ and D meson [61] R_{AA} *vs.* centrality for low p_T (*top*) and high p_T (*middle*). The average N_{part} values correspond to events flatly distributed across centrality. *Bottom* Prompt J/ψ and D meson [31], and charged hadron [58,60] v_2 *vs.* p_T

should have higher v_2 values, closer to those of light-quark hadrons [27].

5.2 Open charm versus beauty

The *top* panel of Fig. 10 shows the R_{AA} dependence on centrality of the nonprompt J/ψ (decay product of B mesons originating from b quarks) and for D mesons (originating from c quarks). The D mesons are more suppressed than the nonprompt J/ψ. This is expected in models that assume less radiative energy loss for the b quark compared to that of a c quark because of the 'dead-cone effect' (the suppression of gluon bremsstrahlung of a quark with mass m and energy E, for angles $\theta < m/E$ [72,73]), and smaller collisional energy loss for the much heavier b quark than for the c quark [15,74]. The results bring extra information in a kinematic phase space not accessible with fully reconstructed b jet measurements, which show that for $p_{\mathrm{T}} > 80\,\mathrm{GeV/c}$ the R_{AA} of b jets is compatible to that of light-quark or gluon jets [75]. However, assessing and quantifying the parton mass dependence of the in-medium phenomena is not trivial: one has to account among other things for different starting kinematics (different unmodified vacuum spectra of the beauty and charm quarks in the medium), and the effect of different fragmentation functions (and extra decay kinematics) [76]. Also, when considering the parton mass dependence, it should be noted that at high-p_{T}, the R_{AA} of D mesons was found to be similar to that of charged pions over a wide range of event centrality [31].

The *bottom* panel of Fig. 10 shows the p_{T} dependence of the measured v_2 for nonprompt J/ψ, prompt D mesons, and charged hadrons. The precision and statistical reach of the present LHC open beauty and charm v_2 results can not answer: (a) at low p_{T}, whether the b quarks, with their mass much larger than that of the charm quarks, participate or not in the collective expansion of the medium as the charm quarks seem to do; (b) at high p_{T}, whether there is a difference in path-length dependence of energy loss between b and c quarks.

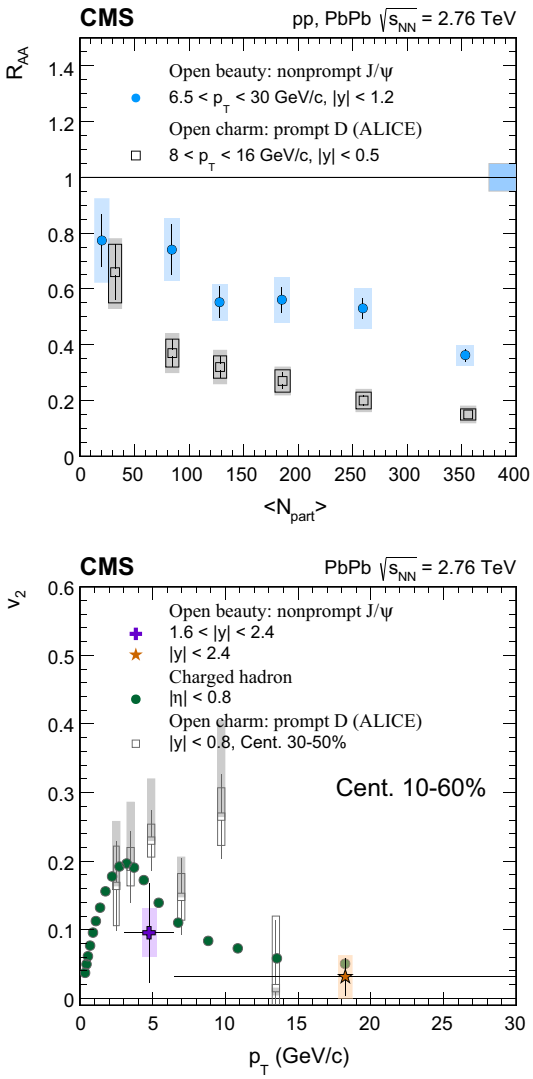

Fig. 10 Nonprompt J/ψ and prompt D meson [31,62], and charged hadron [58,60] R_{AA} *vs.* centrality (*top*), and v_2 *vs.* p_{T} (*bottom*). For the *top* plot, the average N_{part} values correspond to events flatly distributed across centrality

6 Summary

The production of prompt and nonprompt (coming from b hadron decay) J/ψ has been studied in pp and PbPb collisions at $\sqrt{s_{\mathrm{NN}}} = 2.76\,\mathrm{TeV}$. The R_{AA} of the prompt J/ψ mesons, integrated over the rapidity range $|y| < 2.4$ and high p_{T}, $6.5 < p_{\mathrm{T}} < 30\,\mathrm{GeV/c}$, is measured in 12 centrality bins. The R_{AA} is less than unity even in the most peripheral bin, and the suppression becomes steadily stronger as centrality increases. Integrated over rapidity (p_{T}) and centrality, no strong evidence for a p_{T} (rapidity) dependence of the suppression is found. The azimuthal anisotropy of prompt J/ψ mesons shows a nonzero v_2 value in all studied bins, while no strong dependence on centrality, rapidity, or p_{T} is observed.

The R_{AA} of nonprompt J/ψ mesons shows a slow decrease with increasing centrality and rapidity. The results show less suppression at low p_{T}. The first measurement of the nonprompt J/ψ v_2 is also reported in two p_{T} bins for 10–60% event centrality, and the values are consistent with zero elliptical azimuthal anisotropy, though both nominal values are positive.

Acknowledgements We congratulate our colleagues in the CERN accelerator departments for the excellent performance of the LHC and thank the technical and administrative staffs at CERN and at other CMS institutes for their contributions to the success of the CMS effort. In addition, we gratefully acknowledge the computing centres and personnel of the Worldwide LHC Computing Grid for delivering so effec-

tively the computing infrastructure essential to our analyses. Finally, we acknowledge the enduring support for the construction and operation of the LHC and the CMS detector provided by the following funding agencies: the Austrian Federal Ministry of Science, Research and Economy and the Austrian Science Fund; the Belgian Fonds de la Recherche Scientifique, and Fonds voor Wetenschappelijk Onderzoek; the Brazilian Funding Agencies (CNPq, CAPES, FAPERJ, and FAPESP); the Bulgarian Ministry of Education and Science; CERN; the Chinese Academy of Sciences, Ministry of Science and Technology, and National Natural Science Foundation of China; the Colombian Funding Agency (COLCIENCIAS); the Croatian Ministry of Science, Education and Sport, and the Croatian Science Foundation; the Research Promotion Foundation, Cyprus; the Secretariat for Higher Education, Science, Technology and Innovation, Ecuador; the Ministry of Education and Research, Estonian Research Council via IUT23-4 and IUT23-6 and European Regional Development Fund, Estonia; the Academy of Finland, Finnish Ministry of Education and Culture, and Helsinki Institute of Physics; the Institut National de Physique Nucléaire et de Physique des Particules / CNRS, and Commissariat à l'Énergie Atomique et aux Énergies Alternatives / CEA, France; the Bundesministerium für Bildung und Forschung, Deutsche Forschungsgemeinschaft, and Helmholtz-Gemeinschaft Deutscher Forschungszentren, Germany; the General Secretariat for Research and Technology, Greece; the National Scientific Research Foundation, and National Innovation Office, Hungary; the Department of Atomic Energy and the Department of Science and Technology, India; the Institute for Studies in Theoretical Physics and Mathematics, Iran; the Science Foundation, Ireland; the Istituto Nazionale di Fisica Nucleare, Italy; the Ministry of Science, ICT and Future Planning, and National Research Foundation (NRF), Republic of Korea; the Lithuanian Academy of Sciences; the Ministry of Education, and University of Malaya (Malaysia); the Mexican Funding Agencies (BUAP, CINVESTAV, CONACYT, LNS, SEP, and UASLP-FAI); the Ministry of Business, Innovation and Employment, New Zealand; the Pakistan Atomic Energy Commission; the Ministry of Science and Higher Education and the National Science Centre, Poland; the Fundação para a Ciência e a Tecnologia, Portugal; JINR, Dubna; the Ministry of Education and Science of the Russian Federation, the Federal Agency of Atomic Energy of the Russian Federation, Russian Academy of Sciences, and the Russian Foundation for Basic Research; the Ministry of Education, Science and Technological Development of Serbia; the Secretaría de Estado de Investigación, Desarrollo e Innovación and Programa Consolider-Ingenio 2010, Spain; the Swiss Funding Agencies (ETH Board, ETH Zurich, PSI, SNF, UniZH, Canton Zurich, and SER); the Ministry of Science and Technology, Taipei; the Thailand Center of Excellence in Physics, the Institute for the Promotion of Teaching Science and Technology of Thailand, Special Task Force for Activating Research and the National Science and Technology Development Agency of Thailand; the Scientific and Technical Research Council of Turkey, and Turkish Atomic Energy Authority; the National Academy of Sciences of Ukraine, and State Fund for Fundamental Researches, Ukraine; the Science and Technology Facilities Council, UK; the US Department of Energy, and the US National Science Foundation. Individuals have received support from the Marie-Curie programme and the European Research Council and EPLANET (European Union); the Leventis Foundation; the A. P. Sloan Foundation; the Alexander von Humboldt Foundation; the Belgian Federal Science Policy Office; the Fonds pour la Formation à la Recherche dans l'Industrie et dans l'Agriculture (FRIA-Belgium); the Agentschap voor Innovatie door Wetenschap en Technologie (IWT-Belgium); the Ministry of Education, Youth and Sports (MEYS) of the Czech Republic; the Council of Science and Industrial Research, India; the HOMING PLUS programme of the Foundation for Polish Science, cofinanced from European Union, Regional Development Fund, the Mobility Plus programme of the Ministry of Science and Higher Education, the National Science Center (Poland), contracts Harmonia 2014/14/M/ST2/00428, Opus 2013/11/B/ST2/04202, 2014/13/B/ST2/02543 and 2014/15/B/ST2/03998, Sonata-bis 2012/07/E/ST2/01406; the Thalis and Aristeia programmes cofinanced by EU-ESF and the Greek NSRF; the National Priorities Research Program by Qatar National Research Fund; the Programa Clarín-COFUND del Principado de Asturias; the Rachadapisek Sompot Fund for Postdoctoral Fellowship, Chulalongkorn University and the Chulalongkorn Academic into Its 2nd Century Project Advancement Project (Thailand); and the Welch Foundation, contract C-1845.

Funded by SCOAP[3].

A Supplemental Material

The nominator and denominator of the R_{AA}, defined in Eq. (3), and presented in this paper in Figs. 4 and 5 for prompt J/ψ, and Figs. 7 and 8 for nonprompt J/ψ, are tabulated. They represent the efficiency-corrected signal yield within the single muon kinematic region used in this paper. This kinematic region is defined in Eq. (4). These $\sqrt{s_{\mathrm{NN}}} = 2.76\,\mathrm{TeV}$ pp and PbPb fiducial cross sections do not depend on the acceptance, or the associated uncertainties. The corresponding T_{AA} values used in each case are also tabulated.

$$\begin{aligned} &p_{\mathrm{T}}^{\mu} > 3.4\,\mathrm{GeV/c} && \text{for } |\eta^{\mu}| < 1.0, \\ &p_{\mathrm{T}}^{\mu} > (5.8 - 2.4\,|\eta^{\mu}|)\,\mathrm{GeV/c} && \text{for } 1.0 < |\eta^{\mu}| < 1.5, \\ &p_{\mathrm{T}}^{\mu} > (3.4 - 0.78\,|\eta^{\mu}|)\,\mathrm{GeV/c} && \text{for } 1.5 < |\eta^{\mu}| < 2.4. \end{aligned} \quad (4)$$

A.1 Prompt J/ψ

See Tables 1, 2, 3 and 4.

Table 1 The prompt J/ψ fiducial cross section in bins of centrality, measured in PbPb and pp collisions at 2.76 TeV within the muon acceptance defined by Eq. (4), and the nuclear overlap function (T_{AA}, with its systematic uncertainty). Listed uncertainties are statistical first and systematic second. A global systematic uncertainty of 3.2% (3.7%) affects all PbPb (pp) fiducial cross sections. The table corresponds to the top panel of Fig. 4

Centrality (%)	T_{AA} (mb^{-1})	PbPb $\frac{1}{T_{AA}}\frac{d^3N^{J/\psi}_{PbPb}}{dy\,d\langle p_T\rangle\,dCent.}$ (pb/GeV/c)	pp $\frac{d^2\sigma^{J/\psi}_{pp}}{dy\,d\langle p_T\rangle}$ (pb/GeV/c)
$\lvert y\rvert < 2.4$, $6.5 < p_T < 30$ GeV/c			
60–100	0.246 ± 0.041	$50 \pm 3 \pm 9$	$69.6 \pm 0.6 \pm 4.1$
50–60	1.36 ± 0.19	$50 \pm 3 \pm 8$	
45–50	2.29 ± 0.26	$39 \pm 3 \pm 5$	
40–45	3.20 ± 0.34	$38 \pm 2 \pm 5$	
35–40	4.4 ± 0.4	$33 \pm 2 \pm 4$	
30–35	5.8 ± 0.5	$34 \pm 2 \pm 4$	
25–30	7.7 ± 0.5	$32 \pm 1 \pm 4$	
20–25	9.9 ± 0.6	$29 \pm 1 \pm 3$	
15–20	12.7 ± 0.7	$25 \pm 1 \pm 2$	
10–15	16.2 ± 0.8	$21.7 \pm 0.9 \pm 2.3$	
5–10	20.5 ± 0.9	$20.9 \pm 0.8 \pm 1.7$	
0–5	25.9 ± 1.1	$19.6 \pm 0.7 \pm 1.6$	

Table 2 The prompt J/ψ fiducial cross section in bins of absolute rapidity, measured in PbPb and pp collisions at 2.76 TeV within the muon acceptance defined by Eq. (4), and the nuclear overlap function (T_{AA}, with its systematic uncertainty). Listed uncertainties are statistical first and systematic second. A global systematic uncertainty of 6.5% (3.7%) affects all PbPb (pp) fiducial cross sections. The table corresponds to the middle panel of Fig. 4

$\lvert y\rvert$	T_{AA} (mb^{-1})	PbPb $\frac{1}{T_{AA}}\frac{d^2N^{J/\psi}_{PbPb}}{dy\,d\langle p_T\rangle}$ (pb/GeV/c)	pp $\frac{d^2\sigma^{J/\psi}_{pp}}{dy\,d\langle p_T\rangle}$ (pb/GeV/c)
Cent. 0–100%, $6.5 < p_T < 30$ GeV/c			
0.0–0.4	5.67 ± 0.32	$18.1 \pm 0.6 \pm 1.4$	$53 \pm 1 \pm 3$
0.4–0.8		$21.1 \pm 0.7 \pm 1.8$	$57 \pm 1 \pm 4$
0.8–1.2		$28.7 \pm 0.9 \pm 2.0$	$74 \pm 1 \pm 4$
1.2–1.6		$36 \pm 1 \pm 2$	$94 \pm 2 \pm 6$
1.6–2 .0		$38 \pm 1 \pm 3$	$98 \pm 2 \pm 7$
2.0–2.4		$14.4 \pm 0.8 \pm 1.4$	$44 \pm 1 \pm 4$

Table 3 The prompt J/ψ fiducial cross section in bins of p_T, measured in PbPb and pp collisions at 2.76 TeV within the muon acceptance defined by Eq. (4), and the nuclear overlap function (T_{AA}, with its systematic uncertainty). Listed uncertainties are statistical first and systematic second. A global systematic uncertainty of 6.5% (3.7%) affects all PbPb (pp) fiducial cross sections. The table corresponds to the bottom panel of Fig. 4

p_T (GeV/c)	T_{AA} (mb^{-1})	PbPb $\frac{1}{T_{AA}}\frac{d^2N^{J/\psi}_{PbPb}}{dy\,dp_T}$ (pb/GeV/c)	pp $\frac{d^2\sigma^{J/\psi}_{pp}}{dy\,dp_T}$ (pb/GeV/c)
Cent. 0–100%, $1.6 < \lvert y\rvert < 2.4$			
3–4.5	5.67 ± 0.32	$272 \pm 16 \pm 40$	$534 \pm 10 \pm 90$
4.5–5.5		$181 \pm 15 \pm 23$	$478 \pm 10 \pm 41$
5.5–6.5		$137 \pm 7 \pm 14$	$355 \pm 8 \pm 28$
Cent. 0–100%, $\lvert y\rvert < 2.4$			
6.5–8.5	5.67 ± 0.32	$169 \pm 4 \pm 14$	$455 \pm 5 \pm 33$
8.5–9.5		$85 \pm 3 \pm 5$	$252 \pm 5 \pm 15$
9.5–11		$55 \pm 2 \pm 3$	$147 \pm 3 \pm 8$
11–13		$26 \pm 1 \pm 2$	$70 \pm 2 \pm 4$
13–16		$11.5 \pm 0.5 \pm 0.9$	$25.8 \pm 0.8 \pm 1.2$
16–30		$1.25 \pm 0.08 \pm 0.20$	$3.23 \pm 0.14 \pm 0.14$

Table 4 The prompt J/ψ fiducial cross section in bins of centrality, for three $|y|$ and two p_T intervals, measured in PbPb and pp collisions at 2.76 TeV within the muon acceptance defined by Eq. (4), and the nuclear overlap function (T_{AA}, with its systematic uncertainty). Listed uncertainties are statistical first and systematic second. A global systematic uncertainty of 3.2% (3.7%) affects all PbPb (pp) fiducial cross sections. The table corresponds to Fig. 5

Centrality (%)	T_{AA} (mb^{-1})	PbPb $\frac{1}{T_{AA}} \frac{d^3 N^{J/\psi}_{PbPb}}{dy d p_T dCent.}$ (pb/GeV/c)	pp $\frac{d^2\sigma^{J/\psi}_{pp}}{dy d p_T}$ (pb/GeV/c)
$0 < \|y\| < 1.2$, $6.5 < p_T < 30$ GeV/c			
50–100	0.468 ± 0.070	$47 \pm 3 \pm 8$	$61.4 \pm 0.7 \pm 3.7$
40–50	2.75 ± 0.30	$35 \pm 2 \pm 5$	
30–40	5.1 ± 0.4	$31 \pm 2 \pm 4$	
20–30	8.8 ± 0.6	$27 \pm 1 \pm 3$	
10–20	14.5 ± 0.8	$20.0 \pm 0.8 \pm 2.1$	
0–10	23 ± 1	$17.2 \pm 0.7 \pm 1.6$	
$1.2 < \|y\| < 1.6$, $6.5 < p_T < 30$ GeV/c			
50–100	0.468 ± 0.070	$71 \pm 6 \pm 12$	$94 \pm 2 \pm 6$
40–50	2.75 ± 0.30	$55 \pm 5 \pm 7$	
30–40	5.1 ± 0.4	$48 \pm 4 \pm 5$	
20–30	8.8 ± 0.6	$43 \pm 3 \pm 4$	
10–20	14.5 ± 0.8	$30 \pm 2 \pm 3$	
0–10	23 ± 1	$27 \pm 1 \pm 2$	
$1.6 < \|y\| < 2.4$, $6.5 < p_T < 30$ GeV/c			
50–100	0.468 ± 0.070	$46 \pm 4 \pm 8$	$71 \pm 1 \pm 5$
40–50	2.75 ± 0.30	$36 \pm 3 \pm 5$	
30–40	5.1 ± 0.4	$30 \pm 2 \pm 5$	
20–30	8.8 ± 0.6	$28 \pm 2 \pm 3$	
10–20	14.5 ± 0.8	$24 \pm 1 \pm 3$	
0–10	23 ± 1	$22 \pm 1 \pm 2$	
$1.6 < \|y\| < 2.4$, $3 < p_T < 6.5$ GeV/c			
50–100	0.468 ± 0.070	$815 \pm 53 \pm 158$	$1397 \pm 16 \pm 166$
40–50	2.75 ± 0.30	$685 \pm 50 \pm 109$	
30–40	5.1 ± 0.4	$677 \pm 46 \pm 107$	
20–30	8.8 ± 0.6	$572 \pm 35 \pm 85$	
10–20	14.5 ± 0.8	$737 \pm 40 \pm 117$	
0–10	23 ± 1	$508 \pm 29 \pm 92$	

A.2 Nonprompt J/ψ

See Tables 5, 6, 7 and 8.

Table 5 The nonprompt J/ψ fiducial cross section in bins of centrality, measured in PbPb and pp collisions at 2.76 TeV within the muon acceptance defined by Eq. (4), and the nuclear overlap function (T_{AA}, with its systematic uncertainty). Listed uncertainties are statistical first and systematic second. A global systematic uncertainty of 3.2% (3.7%) affects all PbPb (pp) fiducial cross sections. The table corresponds to the top panel of Fig. 7

Centrality (%)	T_{AA} (mb^{-1})	PbPb $\frac{1}{T_{AA}}\frac{d^3N^{J/\psi}_{PbPb}}{dy d p_T dCent.}$ (pb/GeV/c)	pp $\frac{d^2\sigma^{J/\psi}_{pp}}{dy d p_T}$ (pb/GeV/c)
$\lvert y\rvert < 2.4$, $6.5 < p_T < 30$ GeV/c			
50–100	0.468 ± 0.070	$17 \pm 2 \pm 3$	$23.57 \pm 0.33 \pm 1.41$
40–50	2.75 ± 0.30	$16 \pm 1 \pm 2$	
30–40	5.1 ± 0.4	$13 \pm 1 \pm 1$	
20–30	8.8 ± 0.6	$11.9 \pm 0.7 \pm 1.4$	
10–20	14.5 ± 0.8	$10.4 \pm 0.5 \pm 1.3$	
0–10	23 ± 1	$7.8 \pm 0.4 \pm 0.7$	

Table 6 The nonprompt J/ψ fiducial cross section in bins of absolute rapidity, measured in PbPb and pp collisions at 2.76 TeV within the muon acceptance defined by Eq. (4), and the nuclear overlap function (T_{AA}, with its systematic uncertainty). Listed uncertainties are statistical first and systematic second. A global systematic uncertainty of 6.5% (3.7%) affects all PbPb (pp) fiducial cross sections. The table corresponds to the middle panel of Fig. 7

$\lvert y\rvert$	T_{AA} (mb^{-1})	PbPb $\frac{1}{T_{AA}}\frac{d^2N^{J/\psi}_{PbPb}}{dy d p_T}$ (pb/GeV/c)	pp $\frac{d^2\sigma^{J/\psi}_{pp}}{dy d p_T}$ (pb/GeV/c)
Cent. 0–100%, $6.5 < p_T < 30$ GeV/c			
0.0–0.4	5.67 ± 0.32	$10.5 \pm 0.6 \pm 1.3$	$20.0 \pm 0.7 \pm 1.3$
0.4–0.8		$12.1 \pm 0.7 \pm 1.3$	$23.8 \pm 0.8 \pm 1.9$
0.8–1.2		$11.3 \pm 0.6 \pm 0.9$	$25.2 \pm 0.8 \pm 1.4$
1.2–1.6		$13.1 \pm 0.8 \pm 1.2$	$32 \pm 1 \pm 2$
1.6–2.0		$10.7 \pm 0.8 \pm 1.0$	$29 \pm 1 \pm 2$
2.0–2.4		$4.2 \pm 0.5 \pm 0.7$	$12.2 \pm 0.7 \pm 1.2$

Table 7 The nonprompt J/ψ fiducial cross section in bins of p_T, measured in PbPb and pp collisions at 2.76 TeV within the muon acceptance defined by Eq. (4), and the nuclear overlap function (T_{AA}, with its systematic uncertainty). Listed uncertainties are statistical first and systematic second. A global systematic uncertainty of 6.5% (3.7%) affects all PbPb (pp) fiducial cross sections. The table corresponds to the bottom panel of Fig. 7

p_T (GeV/c)	T_{AA} (mb^{-1})	PbPb $\frac{1}{T_{AA}}\frac{d^2N^{J/\psi}_{PbPb}}{dy d p_T}$ (pb/GeV/c)	pp $\frac{d^2\sigma^{J/\psi}_{pp}}{dy d p_T}$ (pb/GeV/c)
Cent. 0–100%, $1.6 < \lvert y\rvert < 2.4$			
3–4.5	5.67 ± 0.32	$46 \pm 7 \pm 8$	$61 \pm 4 \pm 14$
4.5–5.5		$43 \pm 6 \pm 6$	$63 \pm 4 \pm 6$
5.5–6.5		$31 \pm 4 \pm 4$	$57 \pm 3 \pm 5$
Cent. 0–100%, $\lvert y\rvert < 2.4$			
6.5–8.5	5.67 ± 0.32	$52 \pm 3 \pm 4$	$111 \pm 3 \pm 9$
8.5–9.5		$39 \pm 2 \pm 3$	$80 \pm 3 \pm 5$
9.5–11		$22 \pm 1 \pm 1$	$55 \pm 2 \pm 3$
11–13		$16 \pm 1 \pm 2$	$35 \pm 1 \pm 2$
13–16		$6.0 \pm 0.5 \pm 0.8$	$16.3 \pm 0.7 \pm 0.8$
16–30		$1.071 \pm 0.082 \pm 0.203$	$3.04 \pm 0.13 \pm 0.14$

Table 8 The nonprompt J/ψ fiducial cross section in bins of centrality, for three $|y|$ and two p_T intervals, measured in PbPb and pp collisions at 2.76 TeV within the muon acceptance defined by Eq. (4), and the nuclear overlap function (T_{AA}, with its systematic uncertainty). Listed uncertainties are statistical first and systematic second. A global systematic uncertainty of 3.2% (3.7%) affects all PbPb (pp) fiducial cross sections. The table corresponds to Fig. 8

Centrality (%)	T_{AA} (mb^{-1})	PbPb $\frac{1}{T_{AA}}\frac{d^3N^{J/\psi}_{PbPb}}{dy\,d\langle p_T\rangle\,dCent.}$ (pb/GeV/c)	pp $\frac{d^2\sigma^{J/\psi}_{pp}}{dy\,d\langle p_T\rangle}$ (pb/GeV/c)
$0 < \|y\| < 1.2$, $6.5 < p_T < 30$ GeV/c			
50 ± 100	0.468 ± 0.070	18 ± 2 ± 4	23.3 ± 0.4 ± 1.6
40 ± 50	2.75 ± 0.30	17 ± 2 ± 3	
30 ± 40	5.1 ± 0.4	13 ± 1 ± 2	
20 ± 30	8.8 ± 0.6	13 ± 1 ± 2	
10 ± 20	14.5 ± 0.8	12.4 ± 0.8 ± 1.7	
0 ± 10	23 ± 1	8.5 ± 0.5 ± 0.9	
$1.2 < \|y\| < 1.6$, $6.5 < p_T < 30$ GeV/c			
50 ± 100	0.468 ± 0.070	22 ± 4 ± 4	32 ± 1 ± 2
40 ± 50	2.75 ± 0.30	20 ± 4 ± 3	
30 ± 40	5.1 ± 0.4	12 ± 2 ± 1	
20 ± 30	8.8 ± 0.6	15 ± 2 ± 2	
10 ± 20	14.5 ± 0.8	13 ± 1 ± 1	
0 ± 10	23 ± 1	11 ± 1 ± 1	
$1.6 < \|y\| < 2.4$, $6.5 < p_T < 30$ GeV/c			
50 ± 100	0.468 ± 0.070	12 ± 2 ± 2	20.3 ± 0.6 ± 1.5
40 ± 50	2.75 ± 0.30	12 ± 2 ± 2	
30 ± 40	5.1 ± 0.4	13 ± 2 ± 2	
20 ± 30	8.8 ± 0.6	9 ± 1 ± 1	
10 ± 20	14.5 ± 0.8	7.3 ± 0.9 ± 1.1	
0 ± 10	23 ± 1	4.9 ± 0.6 ± 0.7	
$1.6 < \|y\| < 2.4$, $3 < p_T < 6.5$ GeV/c			
50 ± 100	0.468 ± 0.070	163 ± 40 ± 37	179 ± 7 ± 23
40 ± 50	2.75 ± 0.30	192 ± 35 ± 31	
30 ± 40	5.1 ± 0.4	144 ± 29 ± 23	
20 ± 30	8.8 ± 0.6	139 ± 22 ± 20	
10 ± 20	14.5 ± 0.8	120 ± 21 ± 21	
0 ± 10	23 ± 1	101 ± 15 ± 23	

References

1. A. Andronic et al., Heavy-flavour and quarkonium production in the LHC era: from proton–proton to heavy-ion collisions. Eur. Phys. J. C **76**, 107 (2016). doi:10.1140/epjc/s10052-015-3819-5. arXiv:1506.03981
2. E.V. Shuryak, Theory of hadronic plasma. Sov. Phys. JETP **47**, 212 (1978)
3. F. Karsch, E. Laermann, Thermodynamics and in-medium hadron properties from lattice QCD. in *Quark-Gluon Plasma III*, ed. by R.C. Hwa, X.-N. Wang (World Scientific Publishing Co. Pte. Ltd., 2004). arXiv:hep-lat/0305025
4. T. Matsui, H. Satz, J/ψ suppression by quark–gluon plasma formation. Phys. Lett. B **178**, 416 (1986). doi:10.1016/0370-2693(86)91404-8
5. Y.L. Dokshitzer, D.E. Kharzeev, Heavy quark colorimetry of QCD matter. Phys. Lett. B **519**, 199 (2001). doi:10.1016/S0370-2693(01)01130-3. arXiv:hep-ph/0106202
6. LHCb Collaboration, Measurement of J/ψ production in pp collisions at $\sqrt{s} = 7$ TeV. Eur. Phys. J. C **71**, 1645 (2011). doi:10.1140/epjc/s10052-011-1645-y. arXiv:1103.0423
7. CMS Collaboration, Prompt and non-prompt J/ψ production in pp collisions at $\sqrt{s} = 7$ TeV. Eur. Phys. J. C **71**, 1575 (2011). doi:10.1140/epjc/s10052-011-1575-8. arXiv:1011.4193
8. ATLAS Collaboration, Measurement of the differential cross-sections of inclusive, prompt and non-prompt J/ψ production in pp collisions at $\sqrt{s} = 7$ TeV. Nucl. Phys. B **850**, 387 (2011). doi:10.1016/j.nuclphysb.2011.05.015. arXiv:1104.3038
9. Á. Mócsy, P. Petreczky, Color screening melts quarkonium. Phys. Rev. Lett. **99**, 211602 (2007). doi:10.1103/PhysRevLett.99.211602. arXiv:0706.2183
10. E. Braaten, M.H. Thoma, Energy loss of a heavy quark in the quark–gluon plasma. Phys. Rev. D **44**, R2625 (1991). doi:10.1103/PhysRevD.44.R2625

11. B.-W. Zhang, E. Wang, X.-N. Wang, Heavy quark energy loss in nuclear medium. Phys. Rev. Lett. **93**, 072301 (2004). doi:10.1103/PhysRevLett.93.072301. arXiv:nucl-th/0309040
12. N. Armesto, A. Dainese, C.A. Salgado, U.A. Wiedemann, Testing the color charge and mass dependence of parton energy loss with heavy-to-light ratios at BNL RHIC and CERN LHC. Phys. Rev. D **71**, 054027 (2005). doi:10.1103/PhysRevD.71.054027. arXiv:hep-ph/0501225
13. H. van Hees, V. Greco, R. Rapp, Heavy-quark probes of the quark–gluon plasma at RHIC. Phys. Rev. C **73**, 034913 (2006). doi:10.1103/PhysRevC.73.034913. arXiv:nucl-th/0508055
14. S. Peigne, A. Peshier, Collisional energy loss of a fast heavy quark in a quark–gluon plasma. Phys. Rev. D **77**, 114017 (2008). doi:10.1103/PhysRevD.77.114017. arXiv:0802.4364
15. S. Wicks, W. Horowitz, M. Djordjevic, M. Gyulassy, Heavy quark jet quenching with collisional plus radiative energy loss and path length fluctuations. Nucl. Phys. A **783**, 493 (2007). doi:10.1016/j.nuclphysa.2006.11.102. arXiv:nucl-th/0701063
16. P.B. Gossiaux, J. Aichelin, T. Gousset, V. Guiho, Competition of heavy-quark radiative and collisional energy loss in deconfined matter. J. Phys. G **37**, 094019 (2010). doi:10.1088/0954-3899/37/9/094019. arXiv:1001.4166
17. A. Adil, I. Vitev, Collisional dissociation of heavy mesons in dense QCD matter. Phys. Lett. B **649**, 139 (2007). doi:10.1016/j.physletb.2007.03.050. arXiv:hep-ph/0611109
18. R. Sharma, I. Vitev, B.-W. Zhang, Light-cone wave function approach to open heavy flavor dynamics in QCD matter. Phys. Rev. C **80**, 054902 (2009). doi:10.1103/PhysRevC.80.054902. arXiv:0904.0032
19. H. Satz, Calibrating the in-medium behavior of quarkonia. Adv. High Energy Phys. **2013**, 242918 (2013). doi:10.1155/2013/242918. arXiv:1303.3493
20. F. Riek, R. Rapp, Quarkonia and heavy-quark relaxation times in the quark–gluon plasma. Phys. Rev. C **82**, 035201 (2010). doi:10.1103/PhysRevC.82.035201. arXiv:1005.0769
21. R. Sharma, I. Vitev, High transverse momentum quarkonium production and dissociation in heavy ion collisions. Phys. Rev. C **87**, 044905 (2013). doi:10.1103/PhysRevC.87.044905. arXiv:1203.0329
22. CMS Collaboration, Suppression of non-prompt J/ψ, prompt J/ψ, and $\Upsilon(1S)$ in PbPb collisions at $\sqrt{s_{NN}} = 2.76$ TeV. JHEP **05**, 063 (2012). doi:10.1007/JHEP05(2012)063. arXiv:1201.5069
23. ALICE Collaboration, Inclusive, prompt and non-prompt J/ψ production at mid-rapidity in Pb–Pb collisions at $\sqrt{s_{NN}} = 2.76$ TeV. JHEP **07**, 051 (2015). doi:10.1007/JHEP07(2015)051. arXiv:1504.07151
24. ALICE Collaboration, J/ψ suppression at forward rapidity in Pb–Pb collisions at $\sqrt{s_{NN}} = 2.76$ TeV. Phys. Rev. Lett. **109**, 072301 (2012). doi:10.1103/PhysRevLett.109.072301. arXiv:1202.1383
25. PHENIX Collaboration, J/ψ suppression at forward rapidity in AuAu collisions at $\sqrt{s_{NN}} = 200$ GeV. Phys. Rev. C**84**, 054912 (2011). doi:10.1103/PhysRevC.84.054912. arXiv:1103.6269
26. ALICE Collaboration, Differential studies of inclusive J/ψ and $\psi(2S)$ production at forward rapidity in Pb–Pb collisions at $\sqrt{s_{NN}} = 2.76$ TeV. JHEP **05**, 179 (2016). doi:10.1007/JHEP05(2016)179. arXiv:1506.08804
27. X. Zhao, R. Rapp, Medium modifications and production of charmonia at LHC. Nucl. Phys. A **859**, 114 (2011). doi:10.1016/j.nuclphysa.2011.05.001. arXiv:1102.2194
28. A. Andronic, P. Braun-Munzinger, K. Redlich, J. Stachel, The thermal model on the verge of the ultimate test: particle production in Pb–Pb collisions at the LHC. J. Phys. G **38**, 124081 (2011). doi:10.1088/0954-3899/38/12/124081. arXiv:1106.6321
29. E.G. Ferreiro, Charmonium dissociation and recombination at LHC: revisiting comovers. Phys. Lett. B **731**, 57 (2014). doi:10.1016/j.physletb.2014.02.011. arXiv:1210.3209
30. J.-Y. Ollitrault, Anisotropy as a signature of transverse collective flow. Phys. Rev. D **46**, 229 (1992). doi:10.1103/PhysRevD.46.229
31. ALICE Collaboration, Azimuthal anisotropy of D meson production in Pb–Pb collisions at $\sqrt{s_{NN}} = 2.76$ TeV. Phys. Rev. C. **90**, 034904 (2014). doi:10.1103/PhysRevC.90.034904d. arXiv:1405.2001
32. ALICE Collaboration, J/ψ elliptic flow in PbPb collisions at $\sqrt{s_{NN}} = 2.76$ TeV. Phys. Rev. Lett. **111**, 162301 (2013). doi:10.1103/PhysRevLett.111.162301. arXiv:1303.5880
33. P. Braun-Munzinger, J. Stachel, Non)thermal aspects of charmonium production and a new look at J/ψ suppression. Phys. Lett. B **490**, 196 (2000). doi:10.1016/S0370-2693(00)00991-6. arXiv:nucl-th/0007059
34. Y. Liu, Z. Qu, N. Xu, P. Zhuang, J/ψ transverse momentum distribution in high energy nuclear collisions at RHIC. Phys. Lett. B **678**, 72 (2009). doi:10.1016/j.physletb.2009.06.006. arXiv:0901.2757
35. CMS Collaboration, The CMS experiment at the CERN LHC. JINST **3**, S08004 (2008). doi:10.1088/1748-0221/3/08/S08004
36. CMS Collaboration, Observation and studies of jet quenching in PbPb collisions at $\sqrt{s_{NN}} = 2.76$ TeV. Phys. Rev. C **84**, 024906 (2011). doi:10.1103/PhysRevC.84.024906. arXiv:1102.1957
37. CMS Collaboration, Luminosity calibration for the 2013 proton–lead and proton–proton data taking. CMS Physics Analysis Summary CMS-PAS-LUM-13-002, 2013
38. C. Roland, Track reconstruction in heavy ion collisions with the CMS silicon tracker. in *TIME 20005—Proceedings of the 1st Workshop on Tracking in High Multiplicity Environments*. 2006. doi:10.1016/j.nima.2006.05.023. **[Nucl. Instrum. Meth. A 566 (2006) 123]**
39. CMS Collaboration, Description and performance of track and primary-vertex reconstruction with the CMS tracker. JINST **9**, P10009 (2014). doi:10.1088/1748-0221/9/10/P10009. arXiv:1405.6569
40. M.L. Miller, K. Reygers, S.J. Sanders, P. Steinberg, Glauber modeling in high-energy nuclear collisions. Ann. Rev. Nucl. Part. Sci. **57**, 205 (2007). doi:10.1146/annurev.nucl.57.090506.123020. arXiv:nucl-ex/0701025
41. T. Sjöstrand, S. Mrenna, P.Z. Skands, PYTHIA 6.4 physics and manual. JHEP **05**, 026 (2006). doi:10.1088/1126-6708/2006/05/026. arXiv:hep-ph/0603175
42. D.J. Lange, The EvtGen particle decay simulation package. Nucl. Instrum. Methods A **462**, 152 (2001). doi:10.1016/S0168-9002(01)00089-4
43. E. Barberio, Z. Wąs, PHOTOS—a universal Monte Carlo for QED radiative corrections: version 2.0. Comput. Phys. Commun. **79**, 291 (1994). doi:10.1016/0010-4655(94)90074-4
44. ALICE Collaboration, J/ψ polarization in pp collisions at $\sqrt{s} = 7$ TeV. Phys. Rev. Lett. **108**, 082001 (2012). doi:10.1103/PhysRevLett.108.082001. arXiv:1111.1630
45. CMS Collaboration, Measurement of the prompt $/\psi$ and $\psi(2S)$ polarizations in pp collisions at $\sqrt{s} = 7$ TeV. Phys. Lett. B **727**, 381 (2013). doi:10.1016/j.physletb.2013.10.055. arXiv:1307.6070
46. LHCb Collaboration, Measurement of J/ψ polarization in pp collisions at $\sqrt{s} = 7$ TeV. Eur. Phys. J. C **73**, 2631 (2013). doi:10.1140/epjc/s10052-013-2631-3. arXiv:1307.6379
47. CMS Collaboration, Indications of suppression of excited Υ states in PbPb collisions at $\sqrt{s_{NN}} = 2.76$ TeV. Phys. Rev. Lett. **107**, 052302 (2011). doi:10.1103/PhysRevLett.107.052302. arXiv:1105.4894
48. CMS Collaboration, Observation of sequential Upsilon suppression in PbPb collisions. Phys. Rev. Lett. **109**, 222301 (2012). doi:10.1103/PhysRevLett.109.222301. arXiv:1208.2826
49. CMS Collaboration, Event activity dependence of Υ(nS) production in $\sqrt{s_{NN}} = 5.02$ TeV pPb and $\sqrt{s} = 2.76$ TeV pp collisions. JHEP **04**, 103 (2014). doi:10.1007/JHEP04(2014)103. arXiv:1312.6300

50. CMS Collaboration, Measurement of prompt $\psi(2S) \to J/\psi$ yield ratios in PbPb and pp collisions at $\sqrt{s_{NN}} = 2.76$ TeV. Phys. Rev. Lett. **113**, 262301 (2014). doi:10.1103/PhysRevLett.113.262301. arXiv:1410.1804
51. I.P. Lokhtin, A.M. Snigirev, A model of jet quenching in ultrarelativistic heavy ion collisions and high-p_T hadron spectra at RHIC. Eur. Phys. J. C **45**, 211 (2006). doi:10.1140/epjc/s2005-02426-3. arXiv:hep-ph/0506189
52. GEANT4 Collaboration, GEANT4—a simulation toolkit. Nucl. Instrum. Methods A **506**, 250 (2003). doi:10.1016/S0168-9002(03)01368-8
53. CMS Collaboration, Performance of CMS muon reconstruction in pp collision events at $\sqrt{s} = 7$ TeV. JINST **7**, P10002 (2012). doi:10.1088/1748-0221/7/10/P10002. arXiv:1206.4071
54. CMS Collaboration, Dependence on pseudorapidity and centrality of charged hadron production in PbPb collisions at $\sqrt{s_{NN}} = 2.76$ TeV. JHEP **08**, 141 (2011). doi:10.1007/JHEP08(2011)141. arXiv:1107.4800
55. ALEPH Collaboration, Measurement of the anti-B^0 and B^- meson lifetimes. Phys. Lett. B **307**, 194 (1993). doi:10.1016/0370-2693(93)90211-Y. **[Erratum: Phys. Lett. B 325, 537 (1994)]**
56. CMS Collaboration, J/ψ and $\psi(2S)$ production in pp collisions at $\sqrt{s} = 7$ TeV. JHEP **02**, 011 (2012). doi:10.1007/JHEP02(2012)011. arXiv:1111.1557
57. M. Oreglia, A study of the reactions $\psi' \to \gamma\gamma\psi$. PhD thesis, SLAC (1980)
58. CMS Collaboration, Measurement of the elliptic anisotropy of charged particles produced in PbPb collisions at nucleon–nucleon center-of-mass energy = 2.76 TeV. Phys. Rev. C **87**, 014902 (2013). doi:10.1103/PhysRevC.87.014902. arXiv:1204.1409
59. A.M. Poskanzer, S.A. Voloshin, Methods for analyzing anisotropic flow in relativistic nuclear collisions. Phys. Rev. C **58**, 1671 (1998). doi:10.1103/PhysRevC.58.1671. arXiv:nucl-ex/9805001
60. CMS Collaboration, Azimuthal anisotropy of charged particles at high transverse momenta in PbPb collisions at $\sqrt{s_{NN}} = 2.76$ TeV. Phys. Rev. Lett. **109**, 022301 (2012). doi:10.1103/PhysRevLett.109.022301. arXiv:1204.1850
61. ALICE Collaboration, Suppression of high transverse momentum D mesons in central Pb–Pb collisions at $\sqrt{s_{NN}} = 2.76$ TeV. JHEP **09**, 112 (2012). doi:10.1007/JHEP09(2012)112. arXiv:1203.2160
62. ALICE Collaboration, Centrality dependence of high-p_T D meson suppression in Pb–Pb collisions at $\sqrt{s_{NN}} = 2.76$ TeV. JHEP **11**, 205 (2015). doi:10.1007/JHEP11(2015)205. arXiv:1506.06604
63. F. Arleo, R. Kolevatov, S. Peigné, M. Rustamova, Centrality and $p_\perp$ dependence of J/ψ suppression in proton–nucleus collisions from parton energy loss. JHEP **05**, 155 (2013). doi:10.1007/JHEP05(2013)155. arXiv:1304.0901
64. E.G. Ferreiro, Excited charmonium suppression in proton–nucleus collisions as a consequence of comovers. Phys. Lett. B **749**, 98 (2015). doi:10.1016/j.physletb.2015.07.066. arXiv:1411.0549
65. H. Fujii, K. Watanabe, Heavy quark pair production in high energy pA collisions: quarkonium. Nucl. Phys. A **915**, 1 (2013). doi:10.1016/j.nuclphysa.2013.06.011. arXiv:1304.2221
66. ALICE Collaboration, Centrality dependence of inclusive J/ψ production in p–Pb collisions at $\sqrt{s_{NN}} = 5.02$ TeV. JHEP **11**, 127 (2015). doi:10.1007/JHEP11(2015)127. arXiv:1506.08808
67. ALICE Collaboration, Rapidity and transverse-momentum dependence of the inclusive J/ψ nuclear modification factor in p–Pb collisions at $\sqrt{s_{NN}} = 5.02$ TeV. JHEP **06**, 055 (2015). doi:10.1007/JHEP06(2015)055. arXiv:1503.07
68. P. Faccioli, C. Lourenco, J. Seixas, H.K. Woehri, Study of $\psi(2S)$ and χ_c decays as feed-down sources of J/ψ hadroproduction. JHEP **10**, 004 (2008). doi:10.1088/1126-6708/2008/10/004. arXiv:0809.2153
69. LHCb Collaboration, Measurement of the ratio of prompt χ_c to J/ψ production in pp collisions at $\sqrt{s} = 7$ TeV. Phys. Lett. B **718**, 431 (2012). doi:10.1016/j.physletb.2012.10.068. arXiv:1204.1462
70. M. He, R.J. Fries, R. Rapp, Heavy flavor at the Large Hadron Collider in a strong coupling approach. Phys. Lett. B **735**, 445 (2014). doi:10.1016/j.physletb.2014.05.050. arXiv:1401.3817
71. ALICE Collaboration, Transverse momentum dependence of D-meson production in Pb–Pb collisions at $\sqrt{s_{NN}} = 2.76$ TeV. JHEP **03**, 081 (2016). doi:10.1007/JHEP03(2016)081. arXiv:1509.06888
72. Y.L. Dokshitzer, V.A. Khoze, S.I. Troian, On specific QCD properties of heavy quark fragmentation ('dead cone'). J. Phys. G **17**, 1602 (1991). doi:10.1088/0954-3899/17/10/023
73. N. Armesto, C.A. Salgado, U.A. Wiedemann, Medium induced gluon radiation off massive quarks fills the dead cone. Phys. Rev. D **69**, 114003 (2004). doi:10.1103/PhysRevD.69.114003. arXiv:hep-ph/0312106
74. M. Djordjevic, M. Gyulassy, Heavy quark radiative energy loss in QCD matter. Nucl. Phys. A **733**, 265 (2004). doi:10.1016/j.nuclphysa.2003.12.020. arXiv:nucl-th/0310076
75. CMS Collaboration, Evidence of b-jet quenching in PbPb collisions at $\sqrt{s_{NN}} = 2.76$ TeV. Phys. Rev. Lett. **113**, 132301 (2014). doi:10.1103/PhysRevLett.113.132301. arXiv:1312.4198. **[Erratum: Phys. Rev. Lett 115, 029903 (2015)]**
76. M. Djordjevic, Heavy flavor puzzle at LHC: a serendipitous interplay of jet suppression and fragmentation. Phys. Rev. Lett. **112**, 042302 (2014). doi:10.1103/PhysRevLett.112.042302. arXiv:1307.4702

CMS Collaboration

Yerevan Physics Institute, Yerevan, Armenia
V. Khachatryan, A. M. Sirunyan, A. Tumasyan

Institut für Hochenergiephysik, Wien, Austria
W. Adam, E. Asilar, T. Bergauer, J. Brandstetter, E. Brondolin, M. Dragicevic, J. Erö, M. Flechl, M. Friedl, R. Frühwirth[1], V. M. Ghete, C. Hartl, N. Hörmann, J. Hrubec, M. Jeitler[1], A. König, I. Krätschmer, D. Liko, T. Matsushita, I. Mikulec, D. Rabady, N. Rad, B. Rahbaran, H. Rohringer, J. Schieck[1], J. Strauss, W. Waltenberger, C.-E. Wulz[1]

Institute for Nuclear Problems, Minsk, Belarus
O. Dvornikov, V. Makarenko, V. Zykunov

National Centre for Particle and High Energy Physics, Minsk, Belarus
V. Mossolov, N. Shumeiko, J. Suarez Gonzalez

Universiteit Antwerpen, Antwerpen, Belgium
S. Alderweireldt, E. A. De Wolf, X. Janssen, J. Lauwers, M. Van De Klundert, H. Van Haevermaet, P. Van Mechelen, N. Van Remortel, A. Van Spilbeeck

Vrije Universiteit Brussel, Brussel, Belgium
S. Abu Zeid, F. Blekman, J. D'Hondt, N. Daci, I. De Bruyn, K. Deroover, S. Lowette, S. Moortgat, L. Moreels, A. Olbrechts, Q. Python, S. Tavernier, W. Van Doninck, P. Van Mulders, I. Van Parijs

Université Libre de Bruxelles, Bruxelles, Belgium
H. Brun, B. Clerbaux, G. De Lentdecker, H. Delannoy, G. Fasanella, L. Favart, R. Goldouzian, A. Grebenyuk, G. Karapostoli, T. Lenzi, A. Léonard, J. Luetic, T. Maerschalk, A. Marinov, A. Randle-conde, T. Seva, C. Vander Velde, P. Vanlaer, D. Vannerom, R. Yonamine, F. Zenoni, F. Zhang[2]

Ghent University, Ghent, Belgium
A. Cimmino, T. Cornelis, D. Dobur, A. Fagot, G. Garcia, M. Gul, I. Khvastunov, D. Poyraz, S. Salva, R. Schöfbeck, A. Sharma, M. Tytgat, W. Van Driessche, E. Yazgan, N. Zaganidis

Université Catholique de Louvain, Louvain-la-Neuve, Belgium
H. Bakhshiansohi, C. Beluffi[3], O. Bondu, S. Brochet, G. Bruno, A. Caudron, S. De Visscher, C. Delaere, M. Delcourt, B. Francois, A. Giammanco, A. Jafari, P. Jez, M. Komm, G. Krintiras, V. Lemaitre, A. Magitteri, A. Mertens, M. Musich, C. Nuttens, K. Piotrzkowski, L. Quertenmont, M. Selvaggi, M. Vidal Marono, S. Wertz

Université de Mons, Mons, Belgium
N. Beliy

Centro Brasileiro de Pesquisas Fisicas, Rio de Janeiro, Brazil
W. L. Aldá Júnior, F. L. Alves, G. A. Alves, L. Brito, C. Hensel, A. Moraes, M. E. Pol, P. Rebello Teles

Universidade do Estado do Rio de Janeiro, Rio de Janeiro, Brazil
E. Belchior Batista Das Chagas, W. Carvalho, J. Chinellato[4], A. Custódio, E. M. Da Costa, G. G. Da Silveira[5], D. De Jesus Damiao, C. De Oliveira Martins, S. Fonseca De Souza, L. M. Huertas Guativa, H. Malbouisson, D. Matos Figueiredo, C. Mora Herrera, L. Mundim, H. Nogima, W. L. Prado Da Silva, A. Santoro, A. Sznajder, E. J. Tonelli Manganote[4], A. Vilela Pereira

Universidade Estadual Paulista[a], Universidade Federal do ABC[b], São Paulo, Brazil
S. Ahuja[a], C. A. Bernardes[b], S. Dogra[a], T. R. Fernandez Perez Tomei[a], E. M. Gregores[b], P. G. Mercadante[b], C. S. Moon[a], S. F. Novaes[a], Sandra S. Padula[a], D. Romero Abad[b], J. C. Ruiz Vargas

Institute for Nuclear Research and Nuclear Energy, Sofia, Bulgaria
A. Aleksandrov, R. Hadjiiska, P. Iaydjiev, M. Rodozov, S. Stoykova, G. Sultanov, M. Vutova

University of Sofia, Sofia, Bulgaria
A. Dimitrov, I. Glushkov, L. Litov, B. Pavlov, P. Petkov

Beihang University, Beijing, China
W. Fang[6]

Institute of High Energy Physics, Beijing, China
M. Ahmad, J. G. Bian, G. M. Chen, H. S. Chen, M. Chen, Y. Chen[7], T. Cheng, C. H. Jiang, D. Leggat, Z. Liu, F. Romeo, S. M. Shaheen, A. Spiezia, J. Tao, C. Wang, Z. Wang, H. Zhang, J. Zhao

State Key Laboratory of Nuclear Physics and Technology, Peking University, Beijing, China
Y. Ban, G. Chen, Q. Li, S. Liu, Y. Mao, S. J. Qian, D. Wang, Z. Xu

Universidad de Los Andes, Bogota, Colombia
C. Avila, A. Cabrera, L. F. Chaparro Sierra, C. Florez, J. P. Gomez, C. F. González Hernández, J. D. Ruiz Alvarez, J. C. Sanabria

University of Split, Faculty of Electrical Engineering, Mechanical Engineering and Naval Architecture, Split, Croatia
N. Godinovic, D. Lelas, I. Puljak, P. M. Ribeiro Cipriano, T. Sculac

University of Split, Faculty of Science, Split, Croatia
Z. Antunovic, M. Kovac

Institute Rudjer Boskovic, Zagreb, Croatia
V. Brigljevic, D. Ferencek, K. Kadija, S. Micanovic, L. Sudic, T. Susa

University of Cyprus, Nicosia, Cyprus
A. Attikis, G. Mavromanolakis, J. Mousa, C. Nicolaou, F. Ptochos, P. A. Razis, H. Rykaczewski, D. Tsiakkouri

Charles University, Prague, Czech Republic
M. Finger[8], M. Finger Jr.[8]

Universidad San Francisco de Quito, Quito, Ecuador
E. Carrera Jarrin

Academy of Scientific Research and Technology of the Arab Republic of Egypt, Egyptian Network of High Energy Physics, Cairo, Egypt
A. Ellithi Kamel[9], M. A. Mahmoud[10,11], A. Radi[11,12]

National Institute of Chemical Physics and Biophysics, Tallinn, Estonia
M. Kadastik, L. Perrini, M. Raidal, A. Tiko, C. Veelken

Department of Physics, University of Helsinki, Helsinki, Finland
P. Eerola, J. Pekkanen, M. Voutilainen

Helsinki Institute of Physics, Helsinki, Finland
J. Härkönen, T. Järvinen, V. Karimäki, R. Kinnunen, T. Lampén, K. Lassila-Perini, S. Lehti, T. Lindén, P. Luukka, J. Tuominiemi, E. Tuovinen, L. Wendland

Lappeenranta University of Technology, Lappeenranta, Finland
J. Talvitie, T. Tuuva

IRFU, CEA, Université Paris-Saclay, Gif-sur-Yvette, France
M. Besancon, F. Couderc, M. Dejardin, D. Denegri, B. Fabbro, J. L. Faure, C. Favaro, F. Ferri, S. Ganjour, S. Ghosh, A. Givernaud, P. Gras, G. Hamel de Monchenault, P. Jarry, I. Kucher, E. Locci, M. Machet, J. Malcles, J. Rander, A. Rosowsky, M. Titov, A. Zghiche

Laboratoire Leprince-Ringuet, Ecole Polytechnique, IN2P3-CNRS, Palaiseau, France
A. Abdulsalam, I. Antropov, S. Baffioni, F. Beaudette, P. Busson, L. Cadamuro, E. Chapon, C. Charlot, O. Davignon, R. Granier de Cassagnac, M. Jo, S. Lisniak, P. Miné, M. Nguyen, C. Ochando, G. Ortona, P. Paganini, P. Pigard, S. Regnard, R. Salerno, Y. Sirois, T. Strebler, Y. Yilmaz, A. Zabi

Institut Pluridisciplinaire Hubert Curien, Université de Strasbourg, Université de Haute Alsace Mulhouse, CNRS/IN2P3, Strasbourg, France
J.-L. Agram[13], J. Andrea, A. Aubin, D. Bloch, J.-M. Brom, M. Buttignol, E. C. Chabert, N. Chanon, C. Collard, E. Conte[13], X. Coubez, J.-C. Fontaine[13], D. Gelé, U. Goerlach, A.-C. Le Bihan, K. Skovpen, P. Van Hove

Centre de Calcul de l'Institut National de Physique Nucleaire et de Physique des Particules, CNRS/IN2P3, Villeurbanne, France
S. Gadrat

Université de Lyon, Université Claude Bernard Lyon 1, CNRS-IN2P3, Institut de Physique Nucléaire de Lyon, Villeurbanne, France
S. Beauceron, C. Bernet, G. Boudoul, E. Bouvier, C. A. Carrillo Montoya, R. Chierici, D. Contardo, B. Courbon, P. Depasse, H. El Mamouni, J. Fan, J. Fay, S. Gascon, M. Gouzevitch, G. Grenier, B. Ille, F. Lagarde, I. B. Laktineh, M. Lethuillier, L. Mirabito, A. L. Pequegnot, S. Perries, A. Popov[14], D. Sabes, V. Sordini, M. Vander Donckt, P. Verdier, S. Viret

Georgian Technical University, Tbilisi, Georgia
T. Toriashvili[15]

Tbilisi State University, Tbilisi, Georgia
D. Lomidze

RWTH Aachen University, I. Physikalisches Institut, Aachen, Germany
C. Autermann, S. Beranek, L. Feld, A. Heister, M. K. Kiesel, K. Klein, M. Lipinski, A. Ostapchuk, M. Preuten, F. Raupach, S. Schael, C. Schomakers, J. Schulz, T. Verlage, H. Weber, V. Zhukov[14]

RWTH Aachen University, III. Physikalisches Institut A, Aachen, Germany
A. Albert, M. Brodski, E. Dietz-Laursonn, D. Duchardt, M. Endres, M. Erdmann, S. Erdweg, T. Esch, R. Fischer, A. Güth, M. Hamer, T. Hebbeker, C. Heidemann, K. Hoepfner, S. Knutzen, M. Merschmeyer, A. Meyer, P. Millet, S. Mukherjee, M. Olschewski, K. Padeken, T. Pook, M. Radziej, H. Reithler, M. Rieger, F. Scheuch, L. Sonnenschein, D. Teyssier, S. Thüer

RWTH Aachen University, III. Physikalisches Institut B, Aachen, Germany
V. Cherepanov, G. Flügge, B. Kargoll, T. Kress, A. Künsken, J. Lingemann, T. Müller, A. Nehrkorn, A. Nowack, C. Pistone, O. Pooth, A. Stahl[16]

Deutsches Elektronen-Synchrotron, Hamburg, Germany
M. Aldaya Martin, T. Arndt, C. Asawatangtrakuldee, K. Beernaert, O. Behnke, U. Behrens, A. A. Bin Anuar, K. Borras[17], A. Campbell, P. Connor, C. Contreras-Campana, F. Costanza, C. Diez Pardos, G. Dolinska, G. Eckerlin, D. Eckstein, T. Eichhorn, E. Eren, E. Gallo[18], J. Garay Garcia, A. Geiser, A. Gizhko, J. M. Grados Luyando, P. Gunnellini, A. Harb, J. Hauk, M. Hempel[19], H. Jung, A. Kalogeropoulos, O. Karacheban[19], M. Kasemann, J. Keaveney, C. Kleinwort, I. Korol, D. Krücker, W. Lange, A. Lelek, J. Leonard, K. Lipka, A. Lobanov, W. Lohmann[19], R. Mankel, I.-A. Melzer-Pellmann, A. B. Meyer, G. Mittag, J. Mnich, A. Mussgiller, E. Ntomari, D. Pitzl, R. Placakyte, A. Raspereza, B. Roland, M.Ö. Sahin, P. Saxena, T. Schoerner-Sadenius, C. Seitz, S. Spannagel, N. Stefaniuk, G. P. Van Onsem, R. Walsh, C. Wissing

University of Hamburg, Hamburg, Germany
V. Blobel, M. Centis Vignali, A. R. Draeger, T. Dreyer, E. Garutti, D. Gonzalez, J. Haller, M. Hoffmann, A. Junkes, R. Klanner, R. Kogler, N. Kovalchuk, T. Lapsien, T. Lenz, I. Marchesini, D. Marconi, M. Meyer, M. Niedziela, D. Nowatschin, F. Pantaleo[16], T. Peiffer, A. Perieanu, J. Poehlsen, C. Sander, C. Scharf, P. Schleper, A. Schmidt, S. Schumann, J. Schwandt, H. Stadie, G. Steinbrück, F. M. Stober, M. Stöver, H. Tholen, D. Troendle, E. Usai, L. Vanelderen, A. Vanhoefer, B. Vormwald

Institut für Experimentelle Kernphysik, Karlsruhe, Germany
M. Akbiyik, C. Barth, S. Baur, C. Baus, J. Berger, E. Butz, R. Caspart, T. Chwalek, F. Colombo, W. De Boer, A. Dierlamm, S. Fink, B. Freund, R. Friese, M. Giffels, A. Gilbert, P. Goldenzweig, D. Haitz, F. Hartmann[16], S. M. Heindl, U. Husemann, I. Katkov[14], S. Kudella, P. Lobelle Pardo, H. Mildner, M. U. Mozer, Th. Müller, M. Plagge, G. Quast, K. Rabbertz, S. Röcker, F. Roscher, M. Schröder, I. Shvetsov, G. Sieber, H. J. Simonis, R. Ulrich, J. Wagner-Kuhr, S. Wayand, M. Weber, T. Weiler, S. Williamson, C. Wöhrmann, R. Wolf

Institute of Nuclear and Particle Physics (INPP), NCSR Demokritos, Aghia Paraskevi, Greece
G. Anagnostou, G. Daskalakis, T. Geralis, V. A. Giakoumopoulou, A. Kyriakis, D. Loukas, I. Topsis-Giotis

National and Kapodistrian University of Athens, Athens, Greece
S. Kesisoglou, A. Panagiotou, N. Saoulidou, E. Tziaferi

University of Ioánnina, Ioannina, Greece
I. Evangelou, G. Flouris, C. Foudas, P. Kokkas, N. Loukas, N. Manthos, I. Papadopoulos, E. Paradas

MTA-ELTE Lendület CMS Particle and Nuclear Physics Group, Eötvös Loránd University, Budapest, Hungary
N. Filipovic

Wigner Research Centre for Physics, Budapest, Hungary
G. Bencze, C. Hajdu, D. Horvath[20], F. Sikler, V. Veszpremi, G. Vesztergombi[21], A. J. Zsigmond

Institute of Nuclear Research ATOMKI, Debrecen, Hungary
N. Beni, S. Czellar, J. Karancsi[22], A. Makovec, J. Molnar, Z. Szillasi

University of Debrecen, Debrecen, Hungary
M. Bartók[21], P. Raics, Z. L. Trocsanyi, B. Ujvari

National Institute of Science Education and Research, Bhubaneswar, India
S. Bahinipati, S. Choudhury[23], P. Mal, K. Mandal, A. Nayak[24], D. K. Sahoo, N. Sahoo, S. K. Swain

Panjab University, Chandigarh, India
S. Bansal, S. B. Beri, V. Bhatnagar, R. Chawla, U. Bhawandeep, A. K. Kalsi, A. Kaur, M. Kaur, R. Kumar, P. Kumari, A. Mehta, M. Mittal, J. B. Singh, G. Walia

University of Delhi, Delhi, India
Ashok Kumar, A. Bhardwaj, B. C. Choudhary, R. B. Garg, S. Keshri, S. Malhotra, M. Naimuddin, N. Nishu, K. Ranjan, R. Sharma, V. Sharma

Saha Institute of Nuclear Physics, Kolkata, India
R. Bhattacharya, S. Bhattacharya, K. Chatterjee, S. Dey, S. Dutt, S. Dutta, S. Ghosh, N. Majumdar, A. Modak, K. Mondal, S. Mukhopadhyay, S. Nandan, A. Purohit, A. Roy, D. Roy, S. Roy Chowdhury, S. Sarkar, M. Sharan, S. Thakur

Indian Institute of Technology Madras, Madras, India
P. K. Behera

Bhabha Atomic Research Centre, Mumbai, India
R. Chudasama, D. Dutta, V. Jha, V. Kumar, A. K. Mohanty[16], P. K. Netrakanti, L. M. Pant, P. Shukla, A. Topkar

Tata Institute of Fundamental Research-A, Mumbai, India
T. Aziz, S. Dugad, G. Kole, B. Mahakud, S. Mitra, G. B. Mohanty, B. Parida, N. Sur, B. Sutar

Tata Institute of Fundamental Research-B, Mumbai, India
S. Banerjee, S. Bhowmik[25], R. K. Dewanjee, S. Ganguly, M. Guchait, Sa. Jain, S. Kumar, M. Maity[25], G. Majumder, K. Mazumdar, T. Sarkar[25], N. Wickramage[26]

Indian Institute of Science Education and Research (IISER), Pune, India
S. Chauhan, S. Dube, V. Hegde, A. Kapoor, K. Kothekar, S. Pandey, A. Rane, S. Sharma

Institute for Research in Fundamental Sciences (IPM), Tehran, Iran
H. Behnamian, S. Chenarani[27], E. Eskandari Tadavani, S. M. Etesami[27], A. Fahim[28], M. Khakzad, M. Mohammadi Najafabadi, M. Naseri, S. Paktinat Mehdiabadi[29], F. Rezaei Hosseinabadi, B. Safarzadeh[30], M. Zeinali

University College Dublin, Dublin, Ireland
M. Felcini, M. Grunewald

INFN Sezione di Bari[a], Università di Bari[b], Politecnico di Bari[c], Bari, Italy
M. Abbrescia[a,b], C. Calabria[a,b], C. Caputo[a,b], A. Colaleo[a], D. Creanza[a,c], L. Cristella[a,b], N. De Filippis[a,c], M. De Palma[a,b], L. Fiore[a], G. Iaselli[a,c], G. Maggi[a,c], M. Maggi[a], G. Miniello[a,b], S. My[a,b], S. Nuzzo[a,b], A. Pompili[a,b], G. Pugliese[a,c], R. Radogna[a,b], A. Ranieri[a], G. Selvaggi[a,b], L. Silvestris[a,16], R. Venditti[a,b], P. Verwilligen[a]

INFN Sezione di Bologna[a], Università di Bologna[b], Bologna, Italy
G. Abbiendi[a], C. Battilana, D. Bonacorsi[a,b], S. Braibant-Giacomelli[a,b], L. Brigliadori[a,b], R. Campanini[a,b], P. Capiluppi[a,b], A. Castro[a,b], F. R. Cavallo[a], S. S. Chhibra[a,b], G. Codispoti[a,b], M. Cuffiani[a,b], G. M. Dallavalle[a], F. Fabbri[a], A. Fanfani[a,b], D. Fasanella[a,b], P. Giacomelli[a], C. Grandi[a], L. Guiducci[a,b], S. Marcellini[a], G. Masetti[a], A. Montanari[a], F. L. Navarria[a,b], A. Perrotta[a], A. M. Rossi[a,b], T. Rovelli[a,b], G. P. Siroli[a,b], N. Tosi[a,b,16]

INFN Sezione di Catania[a], Università di Catania[b], Catania, Italy
S. Albergo[a,b], S. Costa[a,b], A. Di Mattia[a], F. Giordano[a,b], R. Potenza[a,b], A. Tricomi[a,b], C. Tuve[a,b]

INFN Sezione di Firenze[a], Università di Firenze[b], Firenze, Italy
G. Barbagli[a], V. Ciulli[a,b], C. Civinini[a], R. D'Alessandro[a,b], E. Focardi[a,b], P. Lenzi[a,b], M. Meschini[a], S. Paoletti[a], G. Sguazzoni[a], L. Viliani[a,b,16]

INFN Laboratori Nazionali di Frascati, Frascati, Italy
L. Benussi, S. Bianco, F. Fabbri, D. Piccolo, F. Primavera[16]

INFN Sezione di Genova[a], Università di Genova[b], Genova, Italy
V. Calvelli[a,b], F. Ferro[a], M. Lo Vetere[a,b], M. R. Monge[a,b], E. Robutti[a], S. Tosi[a,b]

INFN Sezione di Milano-Bicocca[a], Università di Milano-Bicocca[b], Milano, Italy
L. Brianza[16], M. E. Dinardo[a,b], S. Fiorendi[a,b,16], S. Gennai[a], A. Ghezzi[a,b], P. Govoni[a,b], M. Malberti, S. Malvezzi[a], R. A. Manzoni[a,b,16], D. Menasce[a], L. Moroni[a], M. Paganoni[a,b], D. Pedrini[a], S. Pigazzini, S. Ragazzi[a,b], T. Tabarelli de Fatis[a,b]

INFN Sezione di Napoli[a], Università di Napoli 'Federico II'[b], Napoli, Italy, Università della Basilicata[c], Potenza, Italy, Università G. Marconi[d], Rome, Italy
S. Buontempo[a], N. Cavallo[a,c], G. De Nardo, S. Di Guida[a,d,16], M. Esposito[a,b], F. Fabozzi[a,c], F. Fienga[a,b], A. O. M. Iorio[a,b], G. Lanza[a], L. Lista[a], S. Meola[a,d,16], P. Paolucci[a,16], C. Sciacca[a,b], F. Thyssen

INFN Sezione di Padova[a], Università di Padova[b], Padova, Italy, Università di Trento[c], Trento, Italy
P. Azzi[a,16], N. Bacchetta[a], L. Benato[a,b], D. Bisello[a,b], A. Boletti[a,b], R. Carlin[a,b], A. Carvalho Antunes De Oliveira[a,b], P. Checchia[a], M. Dall'Osso[a,b], P. De Castro Manzano[a], T. Dorigo[a], U. Dosselli[a], F. Gasparini[a,b], U. Gasparini[a,b], A. Gozzelino[a], S. Lacaprara[a], M. Margoni[a,b], A. T. Meneguzzo[a,b], J. Pazzini[a,b], N. Pozzobon[a,b], P. Ronchese[a,b], F. Simonetto[a,b], E. Torassa[a], M. Zanetti, P. Zotto[a,b], G. Zumerle[a,b]

INFN Sezione di Pavia[a], Università di Pavia[b], Pavia, Italy
A. Braghieri[a], A. Magnani[a,b], P. Montagna[a,b], S. P. Ratti[a,b], V. Re[a], C. Riccardi[a,b], P. Salvini[a], I. Vai[a,b], P. Vitulo[a,b]

INFN Sezione di Perugia[a], Università di Perugia[b], Perugia, Italy
L. Alunni Solestizi[a,b], G. M. Bilei[a], D. Ciangottini[a,b], L. Fanò[a,b], P. Lariccia[a,b], R. Leonardi[a,b], G. Mantovani[a,b], M. Menichelli[a], A. Saha[a], A. Santocchia[a,b]

INFN Sezione di Pisa[a], Università di Pisa[b], Scuola Normale Superiore di Pisa[c], Pisa, Italy
K. Androsov[a,31], P. Azzurri[a,16], G. Bagliesi[a], J. Bernardini[a], T. Boccali[a], R. Castaldi[a], M. A. Ciocci[a,31], R. Dell'Orso[a], S. Donato[a,c], G. Fedi, A. Giassi[a], M. T. Grippo[a,31], F. Ligabue[a,c], T. Lomtadze[a], L. Martini[a,b], A. Messineo[a,b], F. Palla[a], A. Rizzi[a,b], A. Savoy-Navarro[a,32], P. Spagnolo[a], R. Tenchini[a], G. Tonelli[a,b], A. Venturi[a], P. G. Verdini[a]

INFN Sezione di Roma[a], Università di Roma[b], Rome, Italy
L. Barone[a,b], F. Cavallari[a], M. Cipriani[a,b], D. Del Re[a,b,16], M. Diemoz[a], S. Gelli[a,b], E. Longo[a,b], F. Margaroli[a,b], B. Marzocchi[a,b], P. Meridiani[a], G. Organtini[a,b], R. Paramatti[a], F. Preiato[a,b], S. Rahatlou[a,b], C. Rovelli[a], F. Santanastasio[a,b]

INFN Sezione di Torino[a], Università di Torino[b], Torino, Italy, Università del Piemonte Orientale[c], Novara, Italy
N. Amapane[a,b], R. Arcidiacono[a,c,16], S. Argiro[a,b], M. Arneodo[a,c], N. Bartosik[a], R. Bellan[a,b], C. Biino[a], N. Cartiglia[a], F. Cenna[a,b], M. Costa[a,b], R. Covarelli[a,b], A. Degano[a,b], N. Demaria[a], L. Finco[a,b], B. Kiani[a,b], C. Mariotti[a], S. Maselli[a], E. Migliore[a,b], V. Monaco[a,b], E. Monteil[a,b], M. Monteno[a], M. M. Obertino[a,b], L. Pacher[a,b], N. Pastrone[a], M. Pelliccioni[a], G. L. Pinna Angioni[a,b], F. Ravera[a,b], A. Romero[a,b], M. Ruspa[a,c], R. Sacchi[a,b], K. Shchelina[a,b], V. Sola[a], A. Solano[a,b], A. Staiano[a], P. Traczyk[a,b]

INFN Sezione di Trieste[a], Università di Trieste[b], Trieste, Italy
S. Belforte[a], M. Casarsa[a], F. Cossutti[a], G. Della Ricca[a,b], A. Zanetti[a]

Kyungpook National University, Daegu, Korea
D. H. Kim, G. N. Kim, M. S. Kim, S. Lee, S. W. Lee, Y. D. Oh, S. Sekmen, D. C. Son, Y. C. Yang

Chonbuk National University, Jeonju, Korea
A. Lee

Chonnam National University, Institute for Universe and Elementary Particles, Kwangju, Korea
H. Kim, D. H. Moon

Hanyang University, Seoul, Korea
J. A. Brochero Cifuentes, T. J. Kim

Korea University, Seoul, Korea
S. Cho, S. Choi, Y. Go, D. Gyun, S. Ha, B. Hong, Y. Jo, Y. Kim, B. Lee, K. Lee, K. S. Lee, S. Lee, J. Lim, S. K. Park, Y. Roh

Seoul National University, Seoul, Korea
J. Almond, J. Kim, H. Lee, S. B. Oh, B. C. Radburn-Smith, S. H. Seo, U. K. Yang, H. D. Yoo, G. B. Yu

University of Seoul, Seoul, Korea
M. Choi, H. Kim, J. H. Kim, J. S. H. Lee, I. C. Park, G. Ryu, M. S. Ryu

Sungkyunkwan University, Suwon, Korea
Y. Choi, J. Goh, C. Hwang, J. Lee, I. Yu

Vilnius University, Vilnius, Lithuania
V. Dudenas, A. Juodagalvis, J. Vaitkus

National Centre for Particle Physics, Universiti Malaya, Kuala Lumpur, Malaysia
I. Ahmed, Z. A. Ibrahim, J. R. Komaragiri, M. A. B. Md Ali[33], F. Mohamad Idris[34], W. A. T. Wan Abdullah, M. N. Yusli, Z. Zolkapli

Centro de Investigacion y de Estudios Avanzados del IPN, Mexico City, Mexico
H. Castilla-Valdez, E. De La Cruz-Burelo, I. Heredia-De La Cruz[35], A. Hernandez-Almada, R. Lopez-Fernandez, R. Magaña Villalba, J. Mejia Guisao, A. Sanchez-Hernandez

Universidad Iberoamericana, Mexico City, Mexico
S. Carrillo Moreno, C. Oropeza Barrera, F. Vazquez Valencia

Benemerita Universidad Autonoma de Puebla, Puebla, Mexico
S. Carpinteyro, I. Pedraza, H. A. Salazar Ibarguen, C. Uribe Estrada

Universidad Autónoma de San Luis Potosí, San Luis Potosí, Mexico
A. Morelos Pineda

University of Auckland, Auckland, New Zealand
D. Krofcheck

University of Canterbury, Christchurch, New Zealand
P. H. Butler

National Centre for Physics, Quaid-I-Azam University, Islamabad, Pakistan
A. Ahmad, M. Ahmad, Q. Hassan, H. R. Hoorani, W. A. Khan, A. Saddique, M. A. Shah, M. Shoaib, M. Waqas

National Centre for Nuclear Research, Swierk, Poland
H. Bialkowska, M. Bluj, B. Boimska, T. Frueboes, M. Górski, M. Kazana, K. Nawrocki, K. Romanowska-Rybinska, M. Szleper, P. Zalewski

Institute of Experimental Physics, Faculty of Physics, University of Warsaw, Warsaw, Poland
K. Bunkowski, A. Byszuk[36], K. Doroba, A. Kalinowski, M. Konecki, J. Krolikowski, M. Misiura, M. Olszewski, M. Walczak

Laboratório de Instrumentação e Física Experimental de Partículas, Lisboa, Portugal
P. Bargassa, C. Beirão Da Cruz E Silva, B. Calpas, A. Di Francesco, P. Faccioli, P. G. Ferreira Parracho, M. Gallinaro, J. Hollar, N. Leonardo, L. Lloret Iglesias, M. V. Nemallapudi, J. Rodrigues Antunes, J. Seixas, O. Toldaiev, D. Vadruccio, J. Varela, P. Vischia

Joint Institute for Nuclear Research, Dubna, Russia
S. Afanasiev, P. Bunin, M. Gavrilenko, I. Golutvin, I. Gorbunov, A. Kamenev, V. Karjavin, A. Lanev, A. Malakhov, V. Matveev[37,38], V. Palichik, V. Perelygin, S. Shmatov, S. Shulha, N. Skatchkov, V. Smirnov, N. Voytishin, A. Zarubin

Petersburg Nuclear Physics Institute, Gatchina, St. Petersburg, Russia
L. Chtchipounov, V. Golovtsov, Y. Ivanov, V. Kim[39], E. Kuznetsova[40], V. Murzin, V. Oreshkin, V. Sulimov, A. Vorobyev

Institute for Nuclear Research, Moscow, Russia
Yu. Andreev, A. Dermenev, S. Gninenko, N. Golubev, A. Karneyeu, M. Kirsanov, N. Krasnikov, A. Pashenkov, D. Tlisov, A. Toropin

Institute for Theoretical and Experimental Physics, Moscow, Russia
V. Epshteyn, V. Gavrilov, N. Lychkovskaya, V. Popov, I. Pozdnyakov, G. Safronov, A. Spiridonov, M. Toms, E. Vlasov, A. Zhokin

Moscow Institute of Physics and Technology, Dolgoprudny, Russia
A. Bylinkin[38]

National Research Nuclear University 'Moscow Engineering Physics Institute' (MEPhI), Moscow, Russia
R. Chistov[41], S. Polikarpov, V. Rusinov

P.N. Lebedev Physical Institute, Moscow, Russia
V. Andreev, M. Azarkin[38], I. Dremin[38], M. Kirakosyan, A. Leonidov[38], A. Terkulov

Skobeltsyn Institute of Nuclear Physics, Lomonosov Moscow State University, Moscow, Russia
A. Baskakov, A. Belyaev, E. Boos, A. Demiyanov, A. Ershov, A. Gribushin, O. Kodolova, V. Korotkikh, I. Lokhtin, I. Miagkov, S. Obraztsov, S. Petrushanko, V. Savrin, A. Snigirev, I. Vardanyan

Novosibirsk State University (NSU), Novosibirsk, Russia
V. Blinov[42], Y. Skovpen[42], D. Shtol[42]

State Research Center of Russian Federation, Institute for High Energy Physics, Protvino, Russia
I. Azhgirey, I. Bayshev, S. Bitioukov, D. Elumakhov, V. Kachanov, A. Kalinin, D. Konstantinov, V. Krychkine, V. Petrov, R. Ryutin, A. Sobol, S. Troshin, N. Tyurin, A. Uzunian, A. Volkov

University of Belgrade, Faculty of Physics and Vinca Institute of Nuclear Sciences, Belgrade, Serbia
P. Adzic[43], P. Cirkovic, D. Devetak, M. Dordevic, J. Milosevic, V. Rekovic

Centro de Investigaciones Energéticas Medioambientales y Tecnológicas (CIEMAT), Madrid, Spain
J. Alcaraz Maestre, M. Barrio Luna, E. Calvo, M. Cerrada, M. Chamizo Llatas, N. Colino, B. De La Cruz, A. Delgado Peris, A. Escalante Del Valle, C. Fernandez Bedoya, J. P. Fernández Ramos, J. Flix, M. C. Fouz, P. Garcia-Abia, O. Gonzalez Lopez, S. Goy Lopez, J. M. Hernandez, M. I. Josa, E. Navarro De Martino, A. Pérez-Calero Yzquierdo, J. Puerta Pelayo, A. Quintario Olmeda, I. Redondo, L. Romero, M. S. Soares

Universidad Autónoma de Madrid, Madrid, Spain
J. F. de Trocóniz, M. Missiroli, D. Moran

Universidad de Oviedo, Oviedo, Spain
J. Cuevas, J. Fernandez Menendez, I. Gonzalez Caballero, J. R. González Fernández, E. Palencia Cortezon, S. Sanchez Cruz, I. Suárez Andrés, J. M. Vizan Garcia

Instituto de Física de Cantabria (IFCA), CSIC-Universidad de Cantabria, Santander, Spain
I. J. Cabrillo, A. Calderon, J. R. Castiñeiras De Saa, E. Curras, M. Fernandez, J. Garcia-Ferrero, G. Gomez, A. Lopez Virto, J. Marco, C. Martinez Rivero, F. Matorras, J. Piedra Gomez, T. Rodrigo, A. Ruiz-Jimeno, L. Scodellaro, N. Trevisani, I. Vila, R. Vilar Cortabitarte

CERN, European Organization for Nuclear Research, Geneva, Switzerland
D. Abbaneo, E. Auffray, G. Auzinger, M. Bachtis, P. Baillon, A. H. Ball, D. Barney, P. Bloch, A. Bocci, A. Bonato, C. Botta, T. Camporesi, R. Castello, M. Cepeda, G. Cerminara, M. D'Alfonso, D. d'Enterria, A. Dabrowski, V. Daponte, A. David, M. De Gruttola, A. De Roeck, E. Di Marco[44], M. Dobson, B. Dorney, T. du Pree, D. Duggan, M. Dünser, N. Dupont, A. Elliott-Peisert, S. Fartoukh, G. Franzoni, J. Fulcher, W. Funk, D. Gigi, K. Gill, M. Girone, F. Glege, D. Gulhan, S. Gundacker, M. Guthoff, J. Hammer, P. Harris, J. Hegeman, V. Innocente, P. Janot, J. Kieseler, H. Kirschenmann, V. Knünz, A. Kornmayer[16], M. J. Kortelainen, K. Kousouris, M. Krammer[1], C. Lange, P. Lecoq, C. Lourenço, M. T. Lucchini, L. Malgeri, M. Mannelli, A. Martelli, F. Meijers, J. A. Merlin, S. Mersi, E. Meschi, P. Milenovic[45], F. Moortgat, S. Morovic, M. Mulders, H. Neugebauer, S. Orfanelli, L. Orsini, L. Pape, E. Perez, M. Peruzzi, A. Petrilli, G. Petrucciani, A. Pfeiffer, M. Pierini, A. Racz, T. Reis, G. Rolandi[46], M. Rovere, M. Ruan, H. Sakulin, J. B. Sauvan, C. Schäfer, C. Schwick, M. Seidel, A. Sharma, P. Silva, P. Sphicas[47], J. Steggemann, M. Stoye, Y. Takahashi, M. Tosi, D. Treille, A. Triossi, A. Tsirou, V. Veckalns[48], G. I. Veres[21], M. Verweij, N. Wardle, H. K. Wöhri, A. Zagozdzinska[36], W. D. Zeuner

Paul Scherrer Institut, Villigen, Switzerland
W. Bertl, K. Deiters, W. Erdmann, R. Horisberger, Q. Ingram, H. C. Kaestli, D. Kotlinski, U. Langenegger, T. Rohe

Institute for Particle Physics, ETH Zurich, Zurich, Switzerland
F. Bachmair, L. Bäni, L. Bianchini, B. Casal, G. Dissertori, M. Dittmar, M. Donegà, C. Grab, C. Heidegger, D. Hits, J. Hoss, G. Kasieczka, P. Lecomte†, W. Lustermann, B. Mangano, M. Marionneau, P. Martinez Ruiz del Arbol, M. Masciovecchio, M. T. Meinhard, D. Meister, F. Micheli, P. Musella, F. Nessi-Tedaldi, F. Pandolfi, J. Pata, F. Pauss, G. Perrin, L. Perrozzi, M. Quittnat, M. Rossini, M. Schönenberger, A. Starodumov[49], V. R. Tavolaro, K. Theofilatos, R. Wallny

Universität Zürich, Zurich, Switzerland
T. K. Aarrestad, C. Amsler[50], L. Caminada, M. F. Canelli, A. De Cosa, C. Galloni, A. Hinzmann, T. Hreus, B. Kilminster, J. Ngadiuba, D. Pinna, G. Rauco, P. Robmann, D. Salerno, Y. Yang, A. Zucchetta

National Central University, Chung-Li, Taiwan
V. Candelise, T. H. Doan, Sh. Jain, R. Khurana, M. Konyushikhin, C. M. Kuo, W. Lin, Y. J. Lu, A. Pozdnyakov, S. S. Yu

National Taiwan University (NTU), Taipei, Taiwan
Arun Kumar, P. Chang, Y. H. Chang, Y. W. Chang, Y. Chao, K. F. Chen, P. H. Chen, C. Dietz, F. Fiori, W.-S. Hou, Y. Hsiung, Y. F. Liu, R.-S. Lu, M. Miñano Moya, E. Paganis, A. Psallidas, J. F. Tsai, Y. M. Tzeng

Chulalongkorn University, Faculty of Science, Department of Physics, Bangkok, Thailand
B. Asavapibhop, G. Singh, N. Srimanobhas, N. Suwonjandee

Cukurova University, Adana, Turkey
A. Adiguzel, S. Cerci[51], S. Damarseckin, Z. S. Demiroglu, C. Dozen, I. Dumanoglu, S. Girgis, G. Gokbulut, Y. Guler, I. Hos[52], E. E. Kangal[53], O. Kara, A. Kayis Topaksu, U. Kiminsu, M. Oglakci, G. Onengut[54], K. Ozdemir[55], D. Sunar Cerci[51], B. Tali[51], S. Turkcapar, I. S. Zorbakir, C. Zorbilmez

Middle East Technical University, Physics Department, Ankara, Turkey
B. Bilin, S. Bilmis, B. Isildak[56], G. Karapinar[57], M. Yalvac, M. Zeyrek

Bogazici University, Istanbul, Turkey
E. Gülmez, M. Kaya[58], O. Kaya[59], E. A. Yetkin[60], T. Yetkin[61]

Istanbul Technical University, Istanbul, Turkey
A. Cakir, K. Cankocak, S. Sen[62]

Institute for Scintillation Materials of National Academy of Science of Ukraine, Kharkov, Ukraine
B. Grynyov

National Scientific Center, Kharkov Institute of Physics and Technology, Kharkov, Ukraine
L. Levchuk, P. Sorokin

University of Bristol, Bristol, UK
R. Aggleton, F. Ball, L. Beck, J. J. Brooke, D. Burns, E. Clement, D. Cussans, H. Flacher, J. Goldstein, M. Grimes, G. P. Heath, H. F. Heath, J. Jacob, L. Kreczko, C. Lucas, D. M. Newbold[63], S. Paramesvaran, A. Poll, T. Sakuma, S. Seif El Nasr-storey, D. Smith, V. J. Smith

Rutherford Appleton Laboratory, Didcot, UK
A. Belyaev[64], C. Brew, R. M. Brown, L. Calligaris, D. Cieri, D. J. A. Cockerill, J. A. Coughlan, K. Harder, S. Harper, E. Olaiya, D. Petyt, C. H. Shepherd-Themistocleous, A. Thea, I. R. Tomalin, T. Williams

Imperial College, London, UK
M. Baber, R. Bainbridge, O. Buchmuller, A. Bundock, D. Burton, S. Casasso, M. Citron, D. Colling, L. Corpe, P. Dauncey, G. Davies, A. De Wit, M. Della Negra, R. Di Maria, P. Dunne, A. Elwood, D. Futyan, Y. Haddad, G. Hall, G. Iles, T. James, R. Lane, C. Laner, R. Lucas[63], L. Lyons, A.-M. Magnan, S. Malik, L. Mastrolorenzo, J. Nash, A. Nikitenko[49], J. Pela, B. Penning, M. Pesaresi, D. M. Raymond, A. Richards, A. Rose, C. Seez, S. Summers, A. Tapper, K. Uchida, M. Vazquez Acosta[65], T. Virdee[16], J. Wright, S. C. Zenz

Brunel University, Uxbridge, UK
J. E. Cole, P. R. Hobson, A. Khan, P. Kyberd, D. Leslie, I. D. Reid, P. Symonds, L. Teodorescu, M. Turner

Baylor University, Waco, USA
A. Borzou, K. Call, J. Dittmann, K. Hatakeyama, H. Liu, N. Pastika

The University of Alabama, Tuscaloosa, USA
S. I. Cooper, C. Henderson, P. Rumerio, C. West

Boston University, Boston, USA
D. Arcaro, A. Avetisyan, T. Bose, D. Gastler, D. Rankin, C. Richardson, J. Rohlf, L. Sulak, D. Zou

Brown University, Providence, USA
G. Benelli, E. Berry, D. Cutts, A. Garabedian, J. Hakala, U. Heintz, J. M. Hogan, O. Jesus, K. H. M. Kwok, E. Laird, G. Landsberg, Z. Mao, M. Narain, S. Piperov, S. Sagir, E. Spencer, R. Syarif

University of California, Davis, Davis, USA
R. Breedon, G. Breto, D. Burns, M. Calderon De La Barca Sanchez, S. Chauhan, M. Chertok, J. Conway, R. Conway, P. T. Cox, R. Erbacher, C. Flores, G. Funk, M. Gardner, W. Ko, R. Lander, C. Mclean, M. Mulhearn, D. Pellett, J. Pilot, S. Shalhout, J. Smith, M. Squires, D. Stolp, M. Tripathi

University of California, Los Angeles, USA
C. Bravo, R. Cousins, A. Dasgupta, P. Everaerts, A. Florent, J. Hauser, M. Ignatenko, N. Mccoll, D. Saltzberg, C. Schnaible, E. Takasugi, V. Valuev, M. Weber

University of California, Riverside, Riverside, USA
K. Burt, R. Clare, J. Ellison, J. W. Gary, S. M. A. Ghiasi Shirazi, G. Hanson, J. Heilman, P. Jandir, E. Kennedy, F. Lacroix, O. R. Long, M. Olmedo Negrete, M. I. Paneva, A. Shrinivas, W. Si, H. Wei, S. Wimpenny, B. R. Yates

University of California, San Diego, La Jolla, USA
J. G. Branson, G. B. Cerati, S. Cittolin, M. Derdzinski, A. Holzner, D. Klein, V. Krutelyov, J. Letts, I. Macneill, D. Olivito, S. Padhi, M. Pieri, M. Sani, V. Sharma, S. Simon, M. Tadel, A. Vartak, S. Wasserbaech[66], C. Welke, J. Wood, F. Würthwein, A. Yagil, G. Zevi Della Porta

Santa Barbara-Department of Physics, University of California, Santa Barbara, USA
N. Amin, R. Bhan dari, J. Bradmiller-Feld, C. Campagnari, A. Dishaw, V. Dutta, M. Franco Sevilla, C. George, F. Golf, L. Gouskos, J. Gran, R. Heller, J. Incandela, S. D. Mullin, A. Ovcharova, H. Qu, J. Richman, D. Stuart, I. Suarez, J. Yoo

California Institute of Technology, Pasadena, USA
D. Anderson, A. Apresyan, J. Bendavid, A. Bornheim, J. Bunn, Y. Chen, J. Duarte, J. M. Lawhorn, A. Mott, H. B. Newman, C. Pena, M. Spiropulu, J. R. Vlimant, S. Xie, R. Y. Zhu

Carnegie Mellon University, Pittsburgh, USA
M. B. Andrews, V. Azzolini, T. Ferguson, M. Paulini, J. Russ, M. Sun, H. Vogel, I. Vorobiev, M. Weinberg

University of Colorado Boulder, Boulder, USA
J. P. Cumalat, W. T. Ford, F. Jensen, A. Johnson, M. Krohn, T. Mulholland, K. Stenson, S. R. Wagner

Cornell University, Ithaca, USA
J. Alexander, J. Chaves, J. Chu, S. Dittmer, K. Mcdermott, N. Mirman, G. Nicolas Kaufman, J. R. Patterson, A. Rinkevicius, A. Ryd, L. Skinnari, L. Soffi, S. M. Tan, Z. Tao, J. Thom, J. Tucker, P. Wittich, M. Zientek

Fairfield University, Fairfield, USA
D. Winn

Fermi National Accelerator Laboratory, Batavia, USA
S. Abdullin, M. Albrow, G. Apollinari, S. Banerjee, L. A. T. Bauerdick, A. Beretvas, J. Berryhill, P. C. Bhat, G. Bolla, K. Burkett, J. N. Butler, H. W. K. Cheung, F. Chlebana, S. Cihangir†, M. Cremonesi, V. D. Elvira, I. Fisk, J. Freeman, E. Gottschalk, L. Gray, D. Green, S. Grünendahl, O. Gutsche, D. Hare, R. M. Harris, S. Hasegawa, J. Hirschauer, Z. Hu, B. Jayatilaka, S. Jindariani, M. Johnson, U. Joshi, B. Klima, B. Kreis, S. Lammel, J. Linacre, D. Lincoln, R. Lipton, T. Liu, R. Lopes De Sá, J. Lykken, K. Maeshima, N. Magini, J. M. Marraffino, S. Maruyama, D. Mason, P. McBride, P. Merkel, S. Mrenna, S. Nahn, C. Newman-Holmes†, V. O'Dell, K. Pedro, O. Prokofyev, G. Rakness, L. Ristori, E. Sexton-Kennedy, A. Soha, W. J. Spalding, L. Spiegel, S. Stoynev, N. Strobbe, L. Taylor, S. Tkaczyk, N. V. Tran, L. Uplegger, E. W. Vaandering, C. Vernieri, M. Verzocchi, R. Vidal, M. Wang, H. A. Weber, A. Whitbeck, Y. Wu

University of Florida, Gainesville, USA
D. Acosta, P. Avery, P. Bortignon, D. Bourilkov, A. Brinkerhoff, A. Carnes, M. Carver, D. Curry, S. Das, R. D. Field, I. K. Furic, J. Konigsberg, A. Korytov, J. F. Low, P. Ma, K. Matchev, H. Mei, G. Mitselmakher, D. Rank, L. Shchutska, D. Sperka, L. Thomas, J. Wang, S. Wang, J. Yelton

Florida International University, Miami, USA
S. Linn, P. Markowitz, G. Martinez, J. L. Rodriguez

Florida State University, Tallahassee, USA
A. Ackert, J. R. Adams, T. Adams, A. Askew, S. Bein, B. Diamond, S. Hagopian, V. Hagopian, K. F. Johnson, A. Khatiwada, H. Prosper, A. Santra, R. Yohay

Florida Institute of Technology, Melbourne, USA
M. M. Baarmand, V. Bhopatkar, S. Colafranceschi, M. Hohlmann, D. Noonan, T. Roy, F. Yumiceva

University of Illinois at Chicago (UIC), Chicago, USA
M. R. Adams, L. Apanasevich, D. Berry, R. R. Betts, I. Bucinskaite, R. Cavanaugh, O. Evdokimov, L. Gauthier, C. E. Gerber, D. J. Hofman, K. Jung, P. Kurt, C. O'Brien, I. D. Sandoval Gonzalez, P. Turner, N. Varelas, H. Wang, Z. Wu, M. Zakaria, J. Zhang

The University of Iowa, Iowa City, USA
B. Bilki[67], W. Clarida, K. Dilsiz, S. Durgut, R. P. Gandrajula, M. Haytmyradov, V. Khristenko, J.-P. Merlo, H. Mermerkaya[68], A. Mestvirishvili, A. Moeller, J. Nachtman, H. Ogul, Y. Onel, F. Ozok[69], A. Penzo, C. Snyder, E. Tiras, J. Wetzel, K. Yi

Johns Hopkins University, Baltimore, USA
I. Anderson, B. Blumenfeld, A. Cocoros, N. Eminizer, D. Fehling, L. Feng, A. V. Gritsan, P. Maksimovic, C. Martin, M. Osherson, J. Roskes, U. Sarica, M. Swartz, M. Xiao, Y. Xin, C. You

The University of Kansas, Lawrence, USA
A. Al-bataineh, P. Baringer, A. Bean, S. Boren, J. Bowen, C. Bruner, J. Castle, L. Forthomme, R. P. Kenny III, S. Khalil, A. Kropivnitskaya, D. Majumder, W. Mcbrayer, M. Murray, S. Sanders, R. Stringer, J. D. Tapia Takaki, Q. Wang

Kansas State University, Manhattan, USA
A. Ivanov, K. Kaadze, Y. Maravin, A. Mohammadi, L. K. Saini, N. Skhirtladze, S. Toda

Lawrence Livermore National Laboratory, Livermore, USA
F. Rebassoo, D. Wright

University of Maryland, College Park, USA
C. Anelli, A. Baden, O. Baron, A. Belloni, B. Calvert, S. C. Eno, C. Ferraioli, J. A. Gomez, N. J. Hadley, S. Jabeen, R. G. Kellogg, T. Kolberg, J. Kunkle, Y. Lu, A. C. Mignerey, F. Ricci-Tam, Y. H. Shin, A. Skuja, M. B. Tonjes, S. C. Tonwar

Massachusetts Institute of Technology, Cambridge, USA
D. Abercrombie, B. Allen, A. Apyan, R. Barbieri, A. Baty, R. Bi, K. Bierwagen, S. Brandt, W. Busza, I. A. Cali, Z. Demiragli, L. Di Matteo, G. Gomez Ceballos, M. Goncharov, D. Hsu, Y. Iiyama, G. M. Innocenti, M. Klute, D. Kovalskyi, K. Krajczar, Y. S. Lai, Y.-J. Lee, A. Levin, P. D. Luckey, B. Maier, A. C. Marini, C. Mcginn, C. Mironov, S. Narayanan, X. Niu, C. Paus, C. Roland, G. Roland, J. Salfeld-Nebgen, G. S. F. Stephans, K. Sumorok, K. Tatar, M. Varma, D. Velicanu, J. Veverka, J. Wang, T. W. Wang, B. Wyslouch, M. Yang, V. Zhukova

University of Minnesota, Minneapolis, USA
A. C. Benvenuti, R. M. Chatterjee, A. Evans, A. Finkel, A. Gude, P. Hansen, S. Kalafut, S. C. Kao, Y. Kubota, Z. Lesko, J. Mans, S. Nourbakhsh, N. Ruckstuhl, R. Rusack, N. Tambe, J. Turkewitz

University of Mississippi, Oxford, USA
J. G. Acosta, S. Oliveros

University of Nebraska-Lincoln, Lincoln, USA
E. Avdeeva, R. Bartek[70], K. Bloom, D. R. Claes, A. Dominguez[70], C. Fangmeier, R. Gonzalez Suarez, R. Kamalieddin, I. Kravchenko, A. Malta Rodrigues, F. Meier, J. Monroy, J. E. Siado, G. R. Snow, B. Stieger

State University of New York at Buffalo, Buffalo, USA
M. Alyari, J. Dolen, J. George, A. Godshalk, C. Harrington, I. Iashvili, J. Kaisen, A. Kharchilava, A. Kumar, A. Parker, S. Rappoccio, B. Roozbahani

Northeastern University, Boston, USA
G. Alverson, E. Barberis, A. Hortiangtham, A. Massironi, D. M. Morse, D. Nash, T. Orimoto, R. Teixeira De Lima, D. Trocino, R.-J. Wang, D. Wood

Northwestern University, Evanston, USA
S. Bhattacharya, O. Charaf, K. A. Hahn, A. Kubik, A. Kumar, N. Mucia, N. Odell, B. Pollack, M. H. Schmitt, K. Sung, M. Trovato, M. Velasco

University of Notre Dame, Notre Dame, USA
N. Dev, M. Hildreth, K. Hurtado Anampa, C. Jessop, D. J. Karmgard, N. Kellams, K. Lannon, N. Marinelli, F. Meng, C. Mueller, Y. Musienko[37], M. Planer, A. Reinsvold, R. Ruchti, G. Smith, S. Taroni, M. Wayne, M. Wolf, A. Woodard

The Ohio State University, Columbus, USA
J. Alimena, L. Antonelli, B. Bylsma, L. S. Durkin, S. Flowers, B. Francis, A. Hart, C. Hill, R. Hughes, W. Ji, B. Liu, W. Luo, D. Puigh, B. L. Winer, H. W. Wulsin

Princeton University, Princeton, USA
S. Cooperstein, O. Driga, P. Elmer, J. Hardenbrook, P. Hebda, D. Lange, J. Luo, D. Marlow, J. Mc Donald, T. Medvedeva, K. Mei, M. Mooney, J. Olsen, C. Palmer, P. Piroué, D. Stickland, A. Svyatkovskiy, C. Tully, A. Zuranski

University of Puerto Rico, Mayaguez, USA
S. Malik

Purdue University, West Lafayette, USA
A. Barker, V. E. Barnes, S. Folgueras, L. Gutay, M. K. Jha, M. Jones, A. W. Jung, D. H. Miller, N. Neumeister, J. F. Schulte, X. Shi, J. Sun, F. Wang, W. Xie

Purdue University Calumet, Hammond, USA
N. Parashar, J. Stupak

Rice University, Houston, USA
A. Adair, B. Akgun, Z. Chen, K. M. Ecklund, F. J. M. Geurts, M. Guilbaud, W. Li, B. Michlin, M. Northup, B. P. Padley, R. Redjimi, J. Roberts, J. Rorie, Z. Tu, J. Zabel

University of Rochester, Rochester, USA
B. Betchart, A. Bodek, P. de Barbaro, R. Demina, Y. T. Duh, T. Ferbel, M. Galanti, A. Garcia-Bellido, J. Han, O. Hindrichs, A. Khukhunaishvili, K. H. Lo, P. Tan, M. Verzetti

Rutgers, The State University of New Jersey, Piscataway, USA
A. Agapitos, J. P. Chou, E. Contreras-Campana, Y. Gershtein, T. A. Gómez Espinosa, E. Halkiadakis, M. Heindl, D. Hidas, E. Hughes, S. Kaplan, R. Kunnawalkam Elayavalli, S. Kyriacou, A. Lath, K. Nash, H. Saka, S. Salur, S. Schnetzer, D. Sheffield, S. Somalwar, R. Stone, S. Thomas, P. Thomassen, M. Walker

University of Tennessee, Knoxville, USA
A. G. Delannoy, M. Foerster, J. Heideman, G. Riley, K. Rose, S. Spanier, K. Thapa

Texas A&M University, College Station, USA
O. Bouhali[71], A. Celik, M. Dalchenko, M. De Mattia, A. Delgado, S. Dildick, R. Eusebi, J. Gilmore, T. Huang, E. Juska, T. Kamon[72], R. Mueller, Y. Pakhotin, R. Patel, A. Perloff, L. Perniè, D. Rathjens, A. Rose, A. Safonov, A. Tatarinov, K. A. Ulmer

Texas Tech University, Lubbock, USA
N. Akchurin, C. Cowden, J. Damgov, F. De Guio, C. Dragoiu, P. R. Dudero, J. Faulkner, E. Gurpinar, S. Kunori, K. Lamichhane, S. W. Lee, T. Libeiro, T. Peltola, S. Undleeb, I. Volobouev, Z. Wang

Vanderbilt University, Nashville, USA
S. Greene, A. Gurrola, R. Janjam, W. Johns, C. Maguire, A. Melo, H. Ni, P. Sheldon, S. Tuo, J. Velkovska, Q. Xu

University of Virginia, Charlottesville, USA
M. W. Arenton, P. Barria, B. Cox, J. Goodell, R. Hirosky, A. Ledovskoy, H. Li, C. Neu, T. Sinthuprasith, X. Sun, Y. Wang, E. Wolfe, F. Xia

Wayne State University, Detroit, USA
C. Clarke, R. Harr, P. E. Karchin, J. Sturdy

University of Wisconsin-Madison, Madison, WI, USA
D. A. Belknap, J. Buchanan, C. Caillol, S. Dasu, L. Dodd, S. Duric, B. Gomber, M. Grothe, M. Herndon, A. Hervé, P. Klabbers, A. Lanaro, A. Levine, K. Long, R. Loveless, I. Ojalvo, T. Perry, G. A. Pierro, G. Polese, T. Ruggles, A. Savin, N. Smith, W. H. Smith, D. Taylor, N. Woods

† **Deceased**

1: Also at Vienna University of Technology, Vienna, Austria
2: Also at State Key Laboratory of Nuclear Physics and Technology, Peking University, Beijing, China
3: Also at Institut Pluridisciplinaire Hubert Curien, Université de Strasbourg, Université de Haute Alsace Mulhouse, CNRS/IN2P3, Strasbourg, France

4: Also at Universidade Estadual de Campinas, Campinas, Brazil
5: Also at Universidade Federal de Pelotas, Pelotas, Brazil
6: Also at Université Libre de Bruxelles, Bruxelles, Belgium
7: Also at Deutsches Elektronen-Synchrotron, Hamburg, Germany
8: Also at Joint Institute for Nuclear Research, Dubna, Russia
9: Also at Cairo University, Cairo, Egypt
10: Also at Fayoum University, El-Fayoum, Egypt
11: Now at British University in Egypt, Cairo, Egypt
12: Now at Ain Shams University, Cairo, Egypt
13: Also at Université de Haute Alsace, Mulhouse, France
14: Also at Skobeltsyn Institute of Nuclear Physics, Lomonosov Moscow State University, Moscow, Russia
15: Also at Tbilisi State University, Tbilisi, Georgia
16: Also at CERN, European Organization for Nuclear Research, Geneva, Switzerland
17: Also at RWTH Aachen University, III. Physikalisches Institut A, Aachen, Germany
18: Also at University of Hamburg, Hamburg, Germany
19: Also at Brandenburg University of Technology, Cottbus, Germany
20: Also at Institute of Nuclear Research ATOMKI, Debrecen, Hungary
21: Also at MTA-ELTE Lendület CMS Particle and Nuclear Physics Group, Eötvös Loránd University, Budapest, Hungary
22: Also at University of Debrecen, Debrecen, Hungary
23: Also at Indian Institute of Science Education and Research, Bhopal, India
24: Also at Institute of Physics, Bhubaneswar, India
25: Also at University of Visva-Bharati, Santiniketan, India
26: Also at University of Ruhuna, Matara, Sri Lanka
27: Also at Isfahan University of Technology, Isfahan, Iran
28: Also at University of Tehran, Department of Engineering Science, Tehran, Iran
29: Also at Yazd University, Yazd, Iran
30: Also at Plasma Physics Research Center, Science and Research Branch, Islamic Azad University, Tehran, Iran
31: Also at Università degli Studi di Siena, Siena, Italy
32: Also at Purdue University, West Lafayette, USA
33: Also at International Islamic University of Malaysia, Kuala Lumpur, Malaysia
34: Also at Malaysian Nuclear Agency, MOSTI, Kajang, Malaysia
35: Also at Consejo Nacional de Ciencia y Tecnología, Mexico city, Mexico
36: Also at Warsaw University of Technology, Institute of Electronic Systems, Warsaw, Poland
37: Also at Institute for Nuclear Research, Moscow, Russia
38: Now at National Research Nuclear University 'Moscow Engineering Physics Institute' (MEPhI), Moscow, Russia
39: Also at St. Petersburg State Polytechnical University, St. Petersburg, Russia
40: Also at University of Florida, Gainesville, USA
41: Also at P.N. Lebedev Physical Institute, Moscow, Russia
42: Also at Budker Institute of Nuclear Physics, Novosibirsk, Russia
43: Also at Faculty of Physics, University of Belgrade, Belgrade, Serbia
44: Also at INFN Sezione di Roma; Università di Roma, Rome, Italy
45: Also at University of Belgrade, Faculty of Physics and Vinca Institute of Nuclear Sciences, Belgrade, Serbia
46: Also at Scuola Normale e Sezione dell'INFN, Pisa, Italy
47: Also at National and Kapodistrian University of Athens, Athens, Greece
48: Also at Riga Technical University, Riga, Latvia
49: Also at Institute for Theoretical and Experimental Physics, Moscow, Russia
50: Also at Albert Einstein Center for Fundamental Physics, Bern, Switzerland
51: Also at Adiyaman University, Adiyaman, Turkey
52: Also at Istanbul Aydin University, Istanbul, Turkey
53: Also at Mersin University, Mersin, Turkey
54: Also at Cag University, Mersin, Turkey
55: Also at Piri Reis University, Istanbul, Turkey
56: Also at Ozyegin University, Istanbul, Turkey

57: Also at Izmir Institute of Technology, Izmir, Turkey
58: Also at Marmara University, Istanbul, Turkey
59: Also at Kafkas University, Kars, Turkey
60: Also at Istanbul Bilgi University, Istanbul, Turkey
61: Also at Yildiz Technical University, Istanbul, Turkey
62: Also at Hacettepe University, Ankara, Turkey
63: Also at Rutherford Appleton Laboratory, Didcot, UK
64: Also at School of Physics and Astronomy, University of Southampton, Southampton, UK
65: Also at Instituto de Astrofísica de Canarias, La Laguna, Spain
66: Also at Utah Valley University, Orem, USA
67: Also at Argonne National Laboratory, Argonne, USA
68: Also at Erzincan University, Erzincan, Turkey
69: Also at Mimar Sinan University, Istanbul, Istanbul, Turkey
70: Now at The Catholic University of America, Washington, USA
71: Also at Texas A&M University at Qatar, Doha, Qatar
72: Also at Kyungpook National University, Daegu, Korea